NOTE TO USERS

This reproduction is the best copy available.

UNIVERSITY OF CALIFORNIA, SAN DIEGO

SAN DIEGO STATE UNIVERSITY

Funtional Characterization and Theoretical Modeling of the *Caenorhadditis Elegans* Egg-laying Circuit

A dissertation submitted in partial satisfaction of the

requirements for the degree Doctor of Philosophy

in

Biology

by

Mi Zhang

Committee in charge:

University of California, San Diego

Professor William R. Schafer, Chair
Professor Marla Feller
Professor Karen Oegema

San Diego State University

Professor Sanford I. Bernstein
Professor Greg L. Harris

2007

The dissertation of Mi Zhang is approved, and it is acceptable in quality and form for publication on microfilm:

_____

_____

_____

_____

_____

Chair

University of California, San Diego

San Diego State University

2007

DEDICATION

This work is solely dedicated t o my enlightenment teacher, my father.

TABLE OF CONTENTS

LIST OF ABBREVIATIONS

5HT	5-hydroxytryptamine (serotonin)
Ach	acetylcholine
CFP	cyan fluorescent protein
CPG	central pattern generator
Egl	egg-laying defective phenotype
Egl-C	egg-laying constitutive phenope
FaRPs	FMRFamide-related peptides
gf	gain of function mutant allele
HSN	hermaphrodite specific neuron
lf	loss of function mutant allele
mec	mechanical sensing defective
N2	wild-type, Bristol
NGM	nematode growth medium
NOR	the "NOR" logic gate
PLM	PLM posterior machanoreceptor neuron
RT	room temperature
SEM	standard error of the mean
TRP	transient portential receptor
unc	uncoordinated
uv1	uv1 neuroendocrine neuron
VC	VC ventral cord neuron

VGCC	voltage-gated $^{Ca2+Ca2+}$ channel
vm	vulval muscle
vm1	vulval muscle type 1
vm2	vulval muscle type 2
Y/C	yellow/cyan ratio
YC	yellow cameleon
YFP	yellow fluorescent protein

LIST OF FIGURES

ACKNOWLEDGEMENTS

I would like to thank my thesis advisor, Prof. William R. Schafer, for his almost un-boundless support all these years; I would also like to thank Dr. Stanley Shyn, Dr. Rex Kerr, Dr. Hiroshi Suzuki and Dr. Caroline R. Craig for invaluable teachings and help; Finally I have to express my great debt to my friend, Prof. Rainer Breitling, who has been a great inspiration and the ultimate intellectual source to me.

The text of Chapter II will be submitted to a peer review journal. The author list includes Mi Zhang, Samuel H. Chung, Caroline R. Craig, Hiroshi Suzuki, Rex Kerr, Eric Mazur and William R. Schafer. I am the primary author of this part of research. Samuel in Mazur's group performed all laser surgeries on the HSN cell body and axons. Hiroshi developed the worm rotating device employed in HSN and VC simultaneous imaging experiment. The idea of using combined visible and fluorescent microscopy is upon Rex's suggestion. Schafer, Callie and I finished text writing.

This text of Chapter III is a currently submitted draft which format is adapted to this thesis. Yeh E*, Ng S*, Zhang M*, Bouhours M, Wang Y, Hung W, Melnik-Martinez K, Li M, Schafer WR and Zhen M are among the author list of "A voltage-Gated Cation Channel-like Protein NCA-1 and a Novel Protein UNC-80 Regulate Synaptic Activity and Development in C. elegans". I am one of the three co-first authors and did all the neural imaging experiments that showed the NCA channel functions at the excitation spreading from the cell body to synapses in the HSN cell to affect egg-laying behavior.

VITA

2001	B.S., Biology, Tsinghua Universiry, P.R. China
2007	Ph.D., Biology, Joint Doctoral Program San Diego State University & University of California, San Diego

PUBLICATIONS

Yeh E*, Ng S*, **Zhang M***, Bouhours M, Wang Y, Hung W, Melnik-Martinez K, Li M, Schafer WR and Zhen M. A Voltage-Gated Cation Channel-like Protein NCA-1 and a Novel Protein UNC-80 Regulate Synaptic Activity and Development in *C. elegans*. (submitted). * o-first authors.

Zhang M, Chung SH, Craig CR, Suzuki H, Kerr R, Schafer WR. Circuitry level Circuitry level characterization of the egg-laying circuit in *Caenorhadbitis elegans*. (to be submitted).

ABSTRACT OF THE DISSERTATION

Functinal Characterization and Theoretical Modeling of the *Caenorhabditis elegans* Egg-laying Circuit

by

Mi Zhang

Doctor of Philosophy in Biology

University of California, San Diego, 2007

San Diego State University, 2007

Professor William R. Schafer, Chair

The nervous system grants animals the ability to react to the complex and ever-changing environment. The ability of the nervous system to control behavior relies not only on the functional properties of individual neurons, but also on the specific pattern of connections in the neural circuits that make up the brain. This dissertation presents the functional study of a simple circuit, specifically the egg-laying circuit in the nematode *Caenorhabditis elegan*, as a model to understand the principles by which networks of neurons generate behavioral patterns.

We first studied the circuit mechanism for individual egg-laying events using neural imaging and laser microsurgery. Our results indicated that the HSN and VC

motorneurons together with vulval muscles (vm1 and vm2) comprise a core circuit that produces egg-laying events upon activation in the absence of sensory inputs. HSN serves as the command neuron of this core circuit, while the VCs, which are reciprocally connected to HSNs, provide a negative feedback loop as well as redundantly exciting the vulval muscles. The roles of two neurotransmitters expressed in these motorneurons, acetycholine and serotonin, have been investigated by directly monitoring both the activities of neurons in the egg-laying circuit in biosynthetic mutants.

With this information about the functional roles of the egg-laying neurons, the egg-laying circuit provides a nice system for studying the effects of specific receptors and channels on neuronal function. As an example, we characterized a newly cloned novel voltage gated cation channel, NCA-1, and demonstrated its function in cellbody-to-synapse excitation in the HSNs.

Based on our results, we have proposed a theoretical model for how the clustered temporal pattern in the egg-laying behavior is generated in wild type animals. The VCs are suggested to work as "the single egg counter" that is activated by individual egg-laying events and inhibits the command neuron HSN for a short period of about 20 seconds. The uv1 cell may serve as "the cluster egg counter", activated by a cluster of closely spaced egg-laying events and inhibiting HSN activity for a longer time of about 20 minutes. Together, these two pathways could produce the observed clustered temporal pattern by acting as negative regulators acting on different time scales.

CHAPTER I. INTRODUCTION

NEURAL CIRCUIT CONSTRUCTION AND "CIRCUITRY DOCTRINES"

Neural circuits regulating separate functional outputs can differ greatly from each other in their overall architecture, yet may be governed by common logic or recurring themes. For example, one feature commonly found in both invertebrate and vertebrate nervous systems is existence of the central pattern generator (CPG), which governs various behaviors such as locomotion and swimming in leech and breathing in humans (for review, see Grillner, 2003). CPGs are local circuits that are capable of producing rhythmic activities in the absence of, but usually under the modulation of, sensory inputs. Studies of connectivity patterns have identified other candidates for potentially conserved circuit motifs. In *C. elegans*, several connectivity motifs involving two to four neurons have been found to be overrepresented with statistical significance compared with random networks and may potentially underlying certain basic computational processes (Reigl et al., 2004). Among the motifs found in *C. elegans*, many have also been shown to be overrepresented in rat cortex (Song et al., 2005). These findings suggest that there may be underlying rules to neural circuit function that are broadly conserved. If so, studies of simpler systems may help provide a reductionist understanding of the anatomy and functional design of the nervous system.

EGG-LAYING BEHAVIOR AND EXPERIMENTAL ASSAYS

Egg-laying is among the earliest behaviors to be studied in *C. elegans*, due to the fact that it can be easily evaluated. Mutant animals which accumulate excess numbers of

eggs within the uterus as the result of decreased egg-laying are called "egg-laying defective," or Egl. The opposite phenotype, animals which retain fewer eggs in the uterus as a result of hyperactive egg-laying, are called "egg-laying constitutive," or Egl-C. However, these traditional descriptions of egg-laying phenotypes only consider the overall egg-laying rate and ignore the temporal complexity of the egg-laying pattern. Instead of a uniform distribution throughout time, egg-laying shows a clustered pattern, which can be modeled as two random processes (Poisson) with different time constants (Figure 1.1) (Zhou et al., 1998). Several different egg-laying assays can be employed in measuring either the overall egg-laying rate and/or temporal egg-laying patterns. These assays and their appropriate applications are detailed below.

1) Visual assessment of the number of eggs accumulated within the uterus under normal culture conditions. This assay is based on the assumption that the egg production rate in the mutant is comparable to wild type and is only suggested for severe Egl-C and Egl phenotypes, which are not sensitive to egg production rate.

2) Measuring the egg-laying rate in M9 buffer in a 96 well pate format (Trent et al., 1983). This protocol was originally developed to test the ability of stimulants (such as drugs) to overcome the inhibitive effects of high-osmolarity M9 buffer. This assay isn't suggested for Egl-C worms, because these worms contain fewer eggs at the beginning of the assay, which makes the egg-laying rate dependent on egg production instead of neural activity. Likewise, this assay isn't recommended for studies of baseline egg-laying in Egl worms, because like wild type animals they are inhibited by M9, and no differences will be detected (although differences in drug responses may still be measured).

3) Evaluating the developmental stage of newly laid eggs. Embryos continue to develop within the hermaphrodite's uterus following fertilization, and the developmental stage at which they are laid depends on the amount of time they are retained within the uterus. A slower egg-laying rate will result in eggs being retained within the uterus for a longer period of time, and therefore laid at a later developmental stage. Wild type animals usually lay eggs after the 8-cell stage but before the comma stage; Egl worms lay coma stage eggs and Egl-C worms lay eggs before the 8-cell stage (Koelle and Horvitz, 1996).

4) Measurement of egg-laying under normal culture conditions. Individual worms are placed on food-seeded NGM plates for two hours, and the number of eggs laid are counted. This assay has the advantage that the test conditions are exactly the same as the normal physiological conditions under which worms are maintained. However, it requires a large quantity of plates, and thus has not been widely used.

5) Evaluating the temporal pattern of egg-laying . Individual worms are recorded using an automated tracking system for long time periods, usually six hours. Each individual egg-laying event happening during this period is temporally mapped. Intervals between two consecutive egg-laying events are calculated and fitted to the dual Poisson model. Fitted parameters are indicators of how different the mutant is compared to wild type in the temporal pattern (Zhou, 1998 IEEE); $\lambda 1$ is how close egg-laying events are within the active state; $p*\lambda 1$ is how close two consecutive active states are; p represents on average how many egg-laying events happen during each active state (Figure 1). This assay is quite labor intensive, however, it is a comprehensive way to evaluate overall egg-laying behavior and quite sensitive to both subtle Egl and Egl-C phenotypes.

CIRCUITRY MECHANISM OF EGG-LAYING BEHAVIOR

The anatomical structure of the egg-laying circuit has been mapped in *C. elegans*, and consists of the vulval muscles (vm1 and vm2), the hermaphrodite specific motorneurons (HSNs), and the ventral cord motorneuron (VCs) (White et al., 1986). Laser ablations of individual cells or multiple cells in combination have been performed in order to study their function. Here, I briefly review the current knowledge of the egg-laying circuit.

Vulval muscle contractions control the opening of the vulva, which results in egg-laying. The two muscle cell types, vm1 and vm2, each have four mono-myocytes positioned rotationally symmetrically to each other. Their longitudinal sides point toward the center of the vulva, forming a cross shape, a geometry which facilitates the opening of the vulva (Figure 1.2). The eight muscles cells are serially connected to each other through gap junctions, suggesting that synchronized contraction is responsible for vulva opening. However, laser ablation has only established the vm2s as essential for the behavior, not the vm1s, indicating a functional difference between them (M Stern, personal communication). The vm2s are the only vulval muscles innervated by motorneurons, HSNL/R and VC4/5.

HSN is important in maintaining an active level of egg-laying, as its absence in genetically ablated mutant *egl-1* (Chen et al., 2000) worms causes a severe Egl phenotype (Trent 1983;Desai and Horvitz, 1989). Several neurotransmitters are expressed in HSNs, including acetylcholine (ACh), (Duerr et al., 1999) serotonin (5-HT), (Desai et al., 1988a; Horvitz et al., 1982a) and several neuropeptides (Kim and Li, 2004; Schinkmann and Li, 1992). Serotonin is capable of restoring the egg-laying behavior in *egl-1* worms (Trent et

al., 1983) and has been suggested to be the main neurotransmitter used by HSN. However, serotonin null *tph-1* mutant worms show only a slight, if any, Egl phenotype (Kim et al., 2001; Reiner et al., 1995), suggesting that other neurotransmitters in HSN may play a role redundant to serotonin.

Interpretation of VC4/5's role in egg laying has been complicated by contradictory results. On one hand, VC4/5 appear to promote egg-laying behavior, because when they are ablated together with HSN, the ablated worms show a more severe egg-laying phenotype than HSN-only ablated worms. On the other hand, ablating VCs alone causes a slight Egl-C phenotype. Therefore, the VCs appear to have contradictory roles in egg-laying, depending on whether or not HSN is intact. Consistent with this, the VCs have been found to inhibit HSN activity, probably through GAR-2, a G-protein linked acetylcholine receptor expressed on HSN cell membranes (Bany et al., 2003). The VCs express Ach (Duerr et al., 1999) and at least one RF-amide neuropeptide (Schinkmann and Li, 1992) as neurotransmitters. Whether or not serotonin is expressed in VCs has been controversial. The VCs stain positive for serotonin antibodies, but the staining is weak, and one key serotonin biosynthetic enzyme, tryptophan hydroxylase, isn't expressed in VCs (Sze et al., 2000). Therefore, the VCs may not express serotonin themselves, but may instead take up exogenous serotonin released from neighboring HSN cells. Acetylcholine is highly likely to be the main neurotransmitter used by the VCs to inhibit HSN and also to excite vulval muscles, though via different receptors- an idea that requires future experimentation.

Although much information has been acquired from genetic and laser ablation experiments, basic questions remain unclear, including whether or not egg-laying events

are tightly controlled by motorneuron activities, and whether or not the cells discussed above constitute the complete egg-laying circuit. This has been due to a lack of methods available to directly study individual cellular activity. The development of methods such as live calcium imaging and axotomy has made possible the functional studies of the egg-laying circuit presented in this thesis.

The circuit, as described out above, are connected via chemical synapses and are potentially capable of fast communications; there might be other cells which may use endocrines in modulating vulva muscles' activity and egg-laying. One such cell, uv1, is recently identified. Vu1 cells are four epithelial cells, but they may acquire neuronal functions as they have short extentions characteristic of touch processes and express neurotransmitters including tyramine. They have been shown to strongly inhibit egg-laying behavior upon activation from their TRPV touch receptors. They are hypothesized to be inactivated when the egg accumulation is low within the uterus and when inactivated induce the active state of egg-laying behavior.

CELLULAR PHYSIOLOGY IN *CAENORHABDITIS ELEGANS*

Over the last 20 years, *C. elegans* has become an increasingly popular model for behavioral neuroscience, following the creation of a nervous system structural map using serial electron microscopy (White et al., 1986). Detailed functional characterization hasn't been easy, due to a lack of available methods for direct study of neuronal activity. Recent technical breakthroughs, particularly laser axotomy, optical cellular physiology, and electrophysiology of dissected preparations, have finally made the functional characterization of the *C. elegans* nervous system more efficient.

Traditional laser ablation surgery, using nano-second pulses with micrometer precision, can be used to kill whole cells and allows for assessment of an individual cell's function (Bargmann and Avery, 1995). This is particularly useful in *C.elegans*, as most neurons or muscles can be specifically identified from their morphology and position, or by using genetic markers. Recently introduced femto-second laser pulses contain higher power intensity and brings the potential precision to submicrometer level, making it possible to ablate individual axons (Chung et al., 2006; Yanik et al., 2004), and can be used in the functional study of synaptic connections.

Optical cellular physiology is non-invasive and therefore useful for *in vivo* studies. Genetically encoded indicators such as cameleon and synapto-pHluorin allow for monitoring of intracellular Ca^{2+} dynamics and synaptic release events respectively, have been widely used in *C. elegans* . Other types of indicators, for changes in protein kinase A (PKA) activity and membrane voltage, are currently under development (Pieribone et al., 2002; Siegel and Isacoff, 1997; Tsutsui et al., 2001; Zhang et al., 2001). Ca^{2+} imaging using the cameleon protein is probably the most widely used optical method since its introduction in *C. elegans* in 2000, and has been successfully applied to a wide range of muscle and neuronal cell types (Kerr et al., 2000; Suzuki et al., 2003). The ratio-metric nature of the signal makes it a reliable tool by effectively eliminating noise from light intensity changes, which can come from either minor movement of immobilized living animals or the instability of electronic energy sources. Genetic modifications have generated better performing cameleons, and the most recent version iYC3.6 features a larger signal magnitude (3-5 times better than previous versions), a reduced Ca^{2+} buffering effect, and less interference with autonomous cellular

physiological pathways (Truong et al., 2007). As more and better indicators are engineered, these optical methods will be increasingly powerful for neurophysiological studies.

In addition to methods which passively monitor naturally occurring neuronal activities, which can be rare or occur only under specific conditions, methods to actively stimulate or inhibit the activity of specific cells are expected to be highly useful in the functional study of neuronal connectivity. Channelrhodopsin (ChR2) and archaeal light-driven chloride pump (NpHR), capable of cellular excitation and inhibition respectively, were recently engineered and have demonstrated success in *C. elegans* (Zhang et al., 2007). A future challenge is to combine these optical manipulation techniques and monitoring methods for the study of complex circuitry mechanisms.

Traditional electrophysiological methods haven't been easy to use in *C.elegans,* due to the worm's small cell size, and high internal body pressure which makes the dissection necessary for electrophysiology difficult. However, several dissection protocols have been successfully developed recently and used in studies of neurotransmitter receptors (Brockie et al., 2001; Richmond et al., 1999), voltage gated calcium channels (Lee et al., 1997b) and mechanosensory transduction channels (O'Hagan et al., 2005).

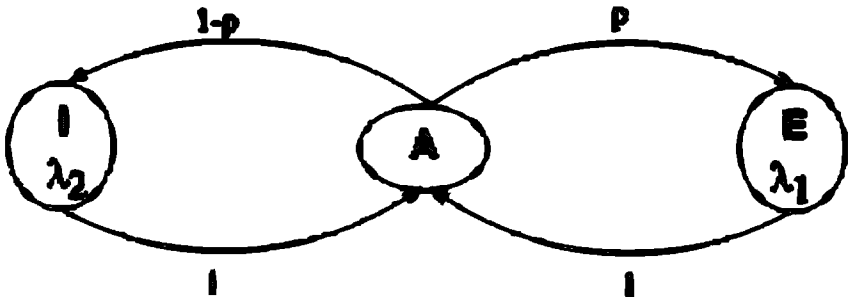

Figure 1.1: Three state model for egg-laying. I = inactive state. A = active state. E = egg-laying state. The A → E transition occurs with probability p, and its time constant is λ1. The A → I transition occurs with probability q = 1-p, and its time constant is λ2. (Zhou et al., 1998)

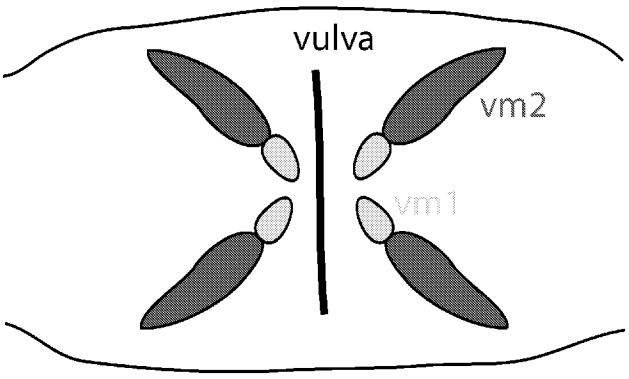

Figure 1.2: The positions of vulval muscles. The vertical black line at the center indicates the vulva. Dark green indicates the vulval muscel type 2 cells (vm2s); Light green indicates the vulval muscle type 1 cells (vm1s).

CHAPTER II. CIRCUITRY LEVEL CHARACTERIZATION OF THE EGG-LAYING CIRCUIT IN *CAENORHABDITIS ELEGANS*

ABSTRACT

Egg-laying in *Caenorhabditis elegans* (*C. elegans*) has been well studied at the genetic, molecular and behavioral levels. However, the roles of specific neurons and the functional nature of the synaptic connections in the egg-laying circuit have remained uncharacterized. We have used *in vivo* neuro-imaging and laser microsurgery to address these questions in intact, behaving animals. We have found that the HSN neurons, which appear to be autonomously active in the absence of synaptic input, play a central role in driving egg-laying behavior through direct excitation of the vulval muscles and VC motorneurons. The VC neurons play a dual role in the egg-laying circuit, exciting the vulval muscles while feedback inhibiting the HSNs. The functional architecture of the egg-laying motor circuit follows a wiring motif that is common in the *C. elegans* nervous system as well as in mammalian cortex; thus the properties of this simple neural circuit may underlie other forms of computation in more complex brains.

INTRODUCTION

How cells in a neural circuit interact to give rise to a behavioral output is a fundamental question for nervous system function. Recent studies have focused on possible circuit mechanisms in a range of neurological abnormalities, including drug addiction and Parkinson's disease (Bergman and Deuschl, 2002; Lesch, 2005); however, the complexity of the neural circuits involved in these disorders has prevented full

elucidation of their underlying neural mechanisms. Several simpler neural circuits have been characterized at the cellular level, including the crustacean stomatogastric ganglion (Marder et al., 2005; Nusbaum and Beenhakker, 2002; Selverston, 2005) and the forward swimming circuits in the leech (Hill et al., 2003) and lamprey (Cangiano and Grillner, 2005; Grillner, 2003; Hellgren et al., 1992). However, none of these model systems is genetically accessible, limiting any study of the molecular machinery that may be conserved among different species and important in human disease. Recent advances in *in vivo* imaging of neural activity in a genetically tractable model organism, the nematode *C. elegans* (Kerr et al., 2000; Suzuki et al., 2003), make possible integrated studies of the genetic, cellular, and circuit-level processes governing behavior.

Among the anatomically simplest neural circuits in *C. elegans* is the one involved in the control of egg-laying behavior. Individual egg-laying events occur through contraction of the vulval muscles, which causes transient opening of the vulva and allows eggs to be expelled. The anatomical structure of the egg-laying circuit directly regulating this activity has been described by White (Figure 2.1A) (White et al., 1986). The circuit is relatively simple, composed of three critical cell types: the vulval muscles (vm1 and vm2), and two pairs of hermaphrodite-specific motorneurons, HSNL/R and VC4/5. Both the HSNs and VCs make neuromuscular synapses with the vm2 vulval muscles; The HSNs make many neuron-to-neuron synapses with the VCs. In addition, there is strong evidence for extrasynaptic connectivity from the VCs to HSNs, as the VCs are cholinergic and the HSNs functionally express the metabotropic Actylcholine receptor (AchR) GAR-2 (Bany et al., 2003). Laser ablation studies have revealed that the vm2 vulval muscles are essential for egg-laying (M. Stern, personal communication). In

addition, ablation of the HSNs severely decreases egg-laying, though egg-laying still occurs at a low frequency (Desai and Horvitz, 1989; Trent et al., 1983). The role of the VCs is more ambiguous, as ablation of the VCs has a weak egg-laying constitutive phenotype on its own but enhances the egg-laying defect of animals lacking the HSNs. Both classes of motorneurons are notable for making use of multiple neurotransmitters and neuromodulators. The HSNs use both acetylcholine (Duerr et al., 1999) and serotonin (Desai et al., 1988b; Horvitz et al., 1982b), as well as severalneuropeptides, *(Kim and Li, 2004; Schinkmann and Li, 1992), (Nathoo et al., 2001).* The VCs are cholinergic (Duerr et al., 1999) and express at least one RF-amide neuropeptide (Schinkmann and Li, 1992). Both acetylcholine and serotonin have been found to have both stimulatory and inhibitory effects on egg-laying (Schafer, 2006), making their study by classical genetic methods quite complicated.

Like most *C. elegans* behaviors, egg-laying is regulated by a diverse set of environmental cues. Egg-laying events occur in a specific temporal pattern (Waggoner et al., 1998b; Zhou et al., 1998) in which eggs are laid in bursts separated by inactive periods averaging 20 minutes in duration. When food is less abundant, these inactive periods become much longer, an effect that requires neuropeptides encoded by the *flp-1* gene (Waggoner et al., 2000b). The neural basis for this modulation by food is not well understood. Vibrational stimulation also inhibits egg-laying; this response has been shown to require the ALM and PLM touch receptor neurons (Sawin, 1996).

Although the putative components of the egg-laying circuitry have been identified, fundamental questions remain about how this circuit controls egg-laying behavior. For example, it is not known whether the synapses between the egg-laying

motorneurons, and their respective synapses with the vulval muscles, are excitatory or inhibitory. Likewise, the functional significance of these connections in the generation of egg-laying behavior is not well understood.

Here, we describe a functional characterization of the neural circuit regulating *C. elegans* egg-laying behavior using *in vivo* calcium imaging. By combining visible light microscopy with *in vivo* calcium imaging, we were able to correlate cellular activity with egg-laying behavior and use genetic and pharmacological manipulations to study the roles of individual neurons and neurotransmitters in the control of egg-laying. In this way, we have been able to define the neural mechanisms by which the core egg-laying circuit generates behavior and trace the neural events from sensation to motor output.

RESULTS

Temporal correlation of egg-laying and motorneuron activity

To obtain more information about the roles of individual muscles and neurons in the egg-laying circuit, we imaged their activities in behaving animals. In a previous study (Shyn et al., 2003), vulval muscle and egg-laying motorneuron activity was imaged in intact immobilized worms; however, the conditions under which these experiments were performed were not permissive for egg-laying. We determined that if animals were immobilized on low osmolarity medium, they laid eggs efficiently under our neuro-imaging conditions. To study egg-laying behavior and neural activity simultaneously, we also developed a technique of combined fluorescence and visible-light microscopy, which allowed us to identify within a single video frame when egg-laying events

occurred, and to correlate these events with calcium transients detected by cameleon expressed in egg-laying neurons or muscle cells (Figure 2.1B).

We first investigated how egg-laying events correlated with the activities of each component of the egg-laying circuit. We observed that all egg-laying events occurred rapidly within a single 100 msecond frame (Figure 2.1B); thus each egg-laying event could be regarded as a point event. In these experiments, we observed that egg-laying events were temporally correlated with Ca^{2+} spikes in both vm1 (n=11/11) and vm2 (n=14/14) vulval muscles (Figure 2.1C). In addition, we also observed strong temporal correlation between egg-laying events and calcium transients in both the HSN (n=15/17) and VC (n=11/12) motorneurons (Figure 2.1C). These results suggest fast excitatory neurotransmission between one or both of these motorneuron classes and the vulval muscles.

We investigated in more detail how osmolarity affected egg-laying behavior and the egg-laying circuitry. By varying the concentrations of ions in the buffer individually and also in combinations, we found that it was the overall osmolarity of the solution, rather than the concentration of a particular ion, that affects the rate of egg-laying (data not shown). We therefore tested dose responses of egg-laying behavior to different osmotic solutions made from sucrose (Figure 2.2A). These results showed gradual, dose-dependent decrease in egg-laying rate as the external osmolarity increased from 10 to 200 mOsmo (M9 is 320mOsm and NGM plates are around150mOsm-180mOsmo). When we performed calcium imaging experiments in high and low osmolarity, we observed that in the HSN and VC neurons, the calcium spike frequencies were likewise high in low osmolarity and silent in high osmolarity conditions (Figure 2.2B, 2.2C), indicating that

osmolarity affects motorneuron activity. We also analyzed the response of the cells in the circuit to an acute osmolarity change from during one continuous 10-min Ca^{2+} imaging recording and observed an activation of HSN and VC activity following the shift to low osmolarity (Figure 2.2D). Together, these results indicate that the regulatory effect of osmolarity on egg-laying involves the control of motorneuron activity.

We also analyzed the effect of osmolarity on vulval muscle activity. Like the HSNs and VCs, the vm1 and vm2 muscles showed higher activity in low osmolarity media (Figure 2.3A, 2.3B), as expected from the higher rate of egg-laying under those conditions. However, even in high osmolarity conditions under which the motorneurons were nearly silent, we observed significant activity (Figure 2.3A, 2.3B) in the vulval muscles suggesting that the muscle cells exhibit spontaneous activity that is motorneuron independent. Interestingly, there was a significant difference in the degree to which the activity of individual vm2 muscle cells was correlated under different osmolarity conditions. Vm2 and vm1s showed 51.9% ($p<0.001$) and 79.62% ($p<0.001$) in correlation in OM10 solution and 14.9% (p isn't significant) and 58.97% ($p<0.001$) in M9. The differences of vm2's self correlations in different conditions also suggest existence of multiple different populations of Ca^{2+} dynamics in it, although there is no obvious kinetic differences detected between them. The self-correlation in vm1s, in contrast, is still preserved in M9 solution; this may be explained by the fact that vm1s are connected to each other through gap junctions whereas vm2s are connected through their gap junctions to vm1s (White et al., 1986).

Interactions between HSN and VC activities

Since HSN and VC activities were both temporally correlated with egg-laying behavior, and since HSNs direct synaptic output to the VCs, we reasoned that HSN activity might likewise be correlated with VC activity. To investigate this possibility directly, we used a rotating device (Hiroshi Suzuki, unpublished) to bring both HSNs and VCs into the same focal plane and image their activity simultaneously. With the tolerance set to 0.1 second, HSN and VC showed 69.9% ($p<0.001$) correlation in the timing of their calcium transients (Figure 2.4A). This close temporal correlation in activity suggests that the HSNs might excite the VCs to drive their activity, or alternatively, that the VCs might excite the HSNs.

To investigate these possibilities, we investigated how eliminating one class of motorneuron affected the activity of the other. We first analyzed *egl-1(n986)* mutants, in which the HSNs specifically and inappropriately undergo programmed cell death in hermaphrodites (Conradt and Horvitz, 1998). We observed that the VC neurons in *egl-1* worms were largely inactive even under low-osmolarity permissive conditions (Figure 4B), suggesting that the HSNs are required to efficiently activate the VCs. We also analyzed *lin-39 (n709ts)* mutant animals (Li and Chalfie, 1990), in which the VC neurons undergo inappropriate cell death. Surprisingly, in these animals the HSN neurons showed increased activity compared to wild-type animals even under inhibitory, high osmolarity conditions (Figure 2.4B). These data suggest that the VCs inhibit, rather than excite, the HSNs.

The *egl-1* and *lin-39* mutant strains also allowed us to determine whether neuromuscular excitation in the egg-laying circuit is mediated by the HSNs, the VCs, or

both. We observed that in *lin-39* mutant animals, which lack VC neurons, egg-laying events were still strongly correlated with HSN activity (Figure 2.4C), suggesting that the synapses from HSN to vulval muscles are excitatory and capable of inducing egg-laying events. Performing the converse experiment in *egl-1* worms was complicated by the fact that these animals have severely defective egg-laying behavior and nearly silent VCs under normally permissive conditions. To surmount this problem, we imaged VCs in *egl-1* worms in the presence of exogenous serotonin, which is known to stimulate egg-laying in the absence of HSN neurons. In the presence of serotonin, VC activity was partially restored, and this activity was temporally coupled with egg-laying events ($p<0.001$) (Figure 2.4C). These results indicated that synapses from VCs to vulval muscles are also excitatory and capable of stimulating egg-laying events. Together, these results suggest that in intact animals, the vulval muscles are redundantly excited by both HSNs and VCs, and that the HSNs stimulate the vulval muscles both directly and indirectly through their excitatory synapses with the VCs.

HSN activity is autonomously generated

We next investigated whether or not HSN activity might be fast excited by other neurons; only the fast excitatory effects are important to the HSN spike timings and therefore for happening egg-laying events also. Most of the synaptic input to the HSNs is directed to its process in the nerve ring, with the exceptions of PLM, PVNR, VC3 and VC5, which send synapses to cell body, right axons and left axon at vulval branches respectively (Figure 2.5B) (White et al., 1986). To determine the effect of the nerve ring input to HSN activity we severed the HSN axons between the nerve ring and the vulva using femtosecond laser axotomy (Figure 2.5A) (Bargmann and Avery, 1995; Chung et

al., 2006; Shen et al., 2005; Yanik et al., 2004). We observe that these ablated animals showed quite active egg-laying behavior (Figure 2.5C), suggesting that the HSNs were still active in these animals. We also ablated either HSN left or right neuron to study the synaptic inputs received by the HSNs from PVNR, VC3 and VC5, respectively. The ablated animals are also quite active, suggesting an active HSN activity in these single HSN ablated worms (Figure 2.5C). The input from PLM has been shown in our later text to be inhibitory to HSN, instead of being excitory, excluding the possibility that the HSN activity is activated by PLM. In contrast, when we ablated the HSN cell bodies using the same equipment, a severe egg-laying defect was observed, consistent with the behavioral phenotype of HSN genetically ablated *egl-1* worms (Figure 2.5C). Altogether the HSNs appear to be solely responsible for individual spike timings, and that inputs from other neurons are either primarily inhibitory or modulatory in nature. Consequently, the HSNs, VCs and vulval muscles may comprise a core egg-laying circuit capable of generating egg-laying behavior in the absence of sensory input.

Effects of serotonin and acetylcholine on the egg-laying circuit

We next investigated the roles of serotonin and acetylcholine, two neurotransmitters that are expressed in the HSN and/or VC motorneurons. Previous neuroimaging studies indicated that exogenous serotonin inhibits HSN activity (Shyn et al., 2003). To further investigate the role of serotonin, we analyzed a mutant defective in the essential serotonin biosynthetic gene *tph-1*. We observed that *tph-1(mg280)* null mutant worms (defective in tryptophan hydroxylase) *(Sze et al., 2000)* showed hyperactivity in the HSN neurons and reduced activity in VCs (Figure 2.6A). Together with our previous finding (Figure 2.3B) that exogenous serotonin stimulates VC activity

in *egl-1* mutants, these results supported the hypothesis that serotonin positively modulates VC activity as well as inhibiting HSN activity.

We next investigated the role of acetylcholine in the egg-laying circuit. Since a complete defect in acetylcholine biosynthesis is lethal, we used a temperature-sensitive allele of the choline acetyltransferase gene, *cha-1 (y226)* (Waggoner et al., 2000a), which upon transfer from 15 to 21°C rapidly undergoes a coiled paralysis characteristic of a strong defect in cholinergic neurotransmission. When we imaged neural activities in the egg-laying circuit approximately 7 minutes following a temperature shift from 15°C to 21°C, we observed significant activity in the HSNs but no activity in the VCs (Figure 2.7A, 2.7B). Moreover, under these conditions egg-laying behavior was strongly reduced (Figure 2.7C). These results suggest that acetylcholine is necessary for excitation of the VCs by the HSNs, and for excitation of the vulval muscles by the HSNs and/or the VCs. Interestingly, longer time, four hours, staying in the restrictive temperature, 21°C, greatly silenced HSN activity (Figure 2.7A, 2.7B), implying that the HSN activity is under the modulation with a slow kinetics of some unidentified endocrine and the acetylcholine may function in that pathway.

Gentle body touch transiently inhibits HSN activity

We were next interested in investigating the neural mechanisms by which egg-laying behavior might be controlled by sensory stimuli. It was shown previously that mechanical vibrations, sensed by the body touch mechanoreceptor neurons, inhibits egg-laying. Since one of these neurons, the posterior touch receptor PLM, directly synapses onto the HSN cell body (White et al., 1986), we wondered whether activation of PLM might affect HSN activity. We stimulated PLM by applying gentle touch stimulation to

the body of an immobilized worm in the posterior body region, which is in the receptive field of PLM but not the other body touch receptors (Suzuki et al., 2003), and imaged HSN activity. As expected, PLM was immediately activated upon mechanical stimulation (Figure 2.8A, 2.8B). In contrast, while HSN showed significant activity before and after touch stimulation, closer analysis of the HSN recording revealed that there was a small but significant increase in the duration of the interval between calcium transients containing the mechanical stimulation compared to mock-stimulated animals ($p<0.05$) (Figure 2.8B). These results indicate that PLM transiently inhibits HSN activity, an effect that may contribute to the inhibition of egg-laying behavior by gentle body touch.

DISCUSSION

Our imaging studies have allowed us to understand more precisely the roles of specific neurons in the egg-laying circuit (Figure 2.9). Of particular importance are the HSN neurons, which affect egg-laying most dramatically when eliminated from the circuit. We observed that HSN activity is highly correlated with egg-laying, even when the VCs have been eliminated, indicating that HSN activity directly evokes individual egg-laying events. The HSNs are also highly correlated in activity with the VCs, and are necessary for VC activation. Thus, the HSNs appear to activate the egg-laying muscles both directly and indirectly through the VCs. Interestingly, HSN activity is independent of sensory or other neuronal input. This suggests that the control of egg-laying is accomplished by modulation of the intrinsic activity of the HSNs.

The HSNs share a number of features with the command neurons of central pattern generators identified in more complex nervous systems. In particular, our

evidence suggests that like classic CPGs, the HSNs are capable of generating patterned motor activity in the absence of sensory input. In addition, the activity of the HSNs is correlated and phasically coupled to the egg-laying motor program. However, while typically CPGs generate rhythmic behavior, the egg-laying circuit generates a behavior whose temporal pattern is aperiodic. Interestingly, it has been suggested that rhythmic CPGs may have evolved from simpler, non-rhythmic neuromodulatory systems (Katz, 1998). The egg-laying motor circuit may represent a novel CPG that generates a patterned but stochastic motor output.

Our results also provided information about the role of the VC motorneurons in the egg-laying circuit. We found that calcium transients in the VCs were dependent on the HSNs and were temporally correlated with HSN calcium transients. These findings lead us to infer that the HSNs excite the VCs. Additionally, VC calcium transients are temporally correlated with egg-laying events, even in the absence of the HSNs; thus, the VCs appear to play a redundant role in exciting the vulval muscles. These data help explain the apparently paradoxical findings that VC ablation can confer either an egg-laying defective or an egg-laying constitutive phenotype, depending on the experimental context. Our results indicating that the VCs negatively regulate egg-laying by inhibiting HSN activity are consistent with previous genetic results indicating the HSNs as a target of negative regulation by the VCs (Bany et al., 2003). Likewise, the apparent redundancy of the VCs stimulatory effect on the vulval muscles is consistent with the earlier observation that VC ablation leads to slower egg-laying most clearly in animals lacking functional HSNs (Waggoner et al., 1998a).

The functional architecture of the egg-laying circuit has intriguing parallels in *C. elegans* as well as in other organisms. A recent analysis found that the connectivity pattern seen in the egg-laying motor circuit, in which two reciprocally-connected cells direct synaptic output to the same target, was significantly overrepresented in the *C. elegans* nervous system. It is thought that such overrepresented motifs may represent functional units, analogous to circuit elements in a computer, that performs key computational functions (Reigl et al., 2004). In the case of the egg-laying circuit, this circuit combines the properties of a negative feedback loop (the HSNs excite the VCs, which in turn feedback inhibit the HSNs) and feed-forward stimulation (the HSNs excite the vulval muscles both directly and indirectly through the VCs). Interestingly, the aforementioned connectivity pattern was recently shown to also be overrepresented in the mammalian cerebral cortex (Song et al., 2005). Thus, studies of the *C. elegans* egg-laying circuit may provide fundamental insights into the properties of microcircuits that underlie the workings of much more complicated brains.

MATERIALS AND METHODS

General Methods and Strains

All nematodes were grown at 20.5±0.5°C on standard Nematode Growth Medium (NGM) seeded with *E. coli* strain OP50 as the food source, except the *cha-1(y226)* temperature sensitive mutant, which was maintained at 15°C. Nematodes were assayed 24 hours after late L4 stage at 20.5±0.5°C, except *cha-1(y226)*, which was assayed 30 hours after later L4 stage. Integrated strains IjIs[N2; myo-3::YC2.0] and ljIs[N2; cat-1::iYC2.1] were generated by gamma irradiation (5000 rad) of existing transgenic lines,

followed by 7 and 6 generations of back-crossing respectively, and did not show obvious differences compared to the wild type N2 strain in egg-laying behavior. Mutant nematode strains, *egl-1(n986), lin-39 (n709ts), tph-1(mg280) and cha-1(y226)*, were crossed to IjIs[N2; myo-3::YC2.0], to generate cameleon lines for Ca^{2+} imaging experiments.

Egg-laying Behavior Assays

Plate egg-laying assays were performed by transferring individual worms to seeded NGM plates and allowing worms to lay eggs for 2 hours before counting the numbers. Liquid egg-laying assays were performed in varying osmolarity conditions in 96-well plates. 100 µl of melted 2% agarose in the indicated buffer were placed in each well and allowed to dry for 1~1.5 hours before starting the behavioral assay. Individual worms were placed on the solid agarose pad in each well and after about 1 min were covered with 50 µl of the same buffer. The number of laid eggs were counted after 15 mins for low osmolarity buffer OM10 (10mM HEPES pH=7.1) or 1 hour for high osmolarity buffer M9.

Ca^{2+} Imaging Experiments

Combined fluorescent and visible microscopy was used to view both the Ca^{2+} signal and egg-laying events simultaneously. The microscope equipment was as described in Suzuki's paper (Suzuki et al., 2003), briefly, a Zeiss Axioskop 2 upright microscope equipped with a Hamamatsu Orca ER CCD camera, a Hamamatsu W-View emission image splitter and a Uniblitz Shutter (Vincent Associates). A minimum of fluorescent light, 20-60% of the original light power with the neutral density filter (ND) of 2.0, was used. Weak visible light, barely revealing egg-laying events, was used to

minimize interference with the cameleon fluorescent signal (as shown in Fig1B). Fluorescent images were acquired and saved using MetaVue 4.6 (Universal Imaging) at a frequency of either 33hz or 10 Hz for muscle and neuron imaging respectively (binning 4X4), using a 63X Zeiss Achroplan water immersion objective.

Worms were immobilized with Nexaband S/C cyanoacrylate veterinary glue on a small agarose pad with the buffer of choice freshly made on a microscopy slide. The worms were then quickly covered with the buffer of choice and immediately moved under the microscope for recording. For HSN and vulval muscle imaging, the agarose pad was made in the same buffer as the bath. For VC imaging, a 2% agarose pad in M9 was used, regardless of the bath buffer, due to the fast adaptation of VCs to low osmolarity conditions. Agarose pads were made immediately before slide preparation in order to minimize the loss of focus in long recordings (10 mins), which usually is caused by swelling of the agarose pad. Worms were allowed to equilibrate for two-four mins before the start of recording.

Bath Flow Setting

A flow chamber was created by connecting a small reservoir (RC-26GLP, Warner Instruments) to inflow buffer and vacuum lines, which allowed for continuous buffer exchange. The chamber was originally filled with 1 ml of the starting buffer and gradually changed over 1~2 mins (flow rate of about 0.3~0.4 ml/min) to the new buffer after the syringe and vacuum connections were opened at the indicated time, 30 seconds after the recording begins.

Serotonin Treatment

10 mg/ml serotonin in 2% agarose M9 buffer was prepared the day of the experiment. 100 µl of the serotonin agarose solution were placed into 96 well plates at room temperature and were allowed to dry for 1.5 hours. Single worms were transferred onto the serotonin agarose pads and covered with 50 µl of 10 mg/ml serotonin in M9 buffer for 30 mins before Ca^{2+} imaging.

Femtosecond Laser Ablation of HSN cell bodies and Axons

Femtosecond laser ablation of the HSN neurons was performed on young adult worms using established procedures. Young adult worms were anesthetized using 1.5 mM sodium azide and imaged on an epi-fluorescent microscope for surgery. A regeneratively-amplified Titanium:sapphire laser (□= 800 nm) delivered a 10 kHz train of 80-90 fs pulses, which were attenuated to 2-3 nJ pulse energy and tightly focused by a 1.4-NA, 63x oil-immersion objective onto the GFP-fluorescent HSN neurons. HSN axons were severed by irradiation for less than 0.5 s, typically at a location half way between the cell body and the nerve ring. HSN cell bodies were ablated by irradiation of the soma two or three times for 1 s. Usually the disappearance of only the nuclear fluorescence was noted within the first second of irradiation.

Microscopic PLM activation

Experiments were performed as in Suzuki's paper (Suzuki et al., 2003). Briefly, a smooth glass rod about 15 um in diameter was mounted on a three-axis manipulator through a M-111.1DG microtranslation stage (Polytec PI) and positioned perpendicular to and barely touching the ventral side of an immobilized worm, about 5-10 um anterior

to the PLM cell body. A 3-second buzz stimulus, 10 um of body shape deflection at10 Hz, was delivered. A LED light flashed once to indicate the beginning of the stimulation.

ACKNOWLEDGEMENTS

We would like to thank Prof. Peter Swoboda (Karolinska Institue, Department of Biosciences and Nutrition, Södertörn University College) for data analysis discussions and Prof. Rainer Breitling (Groningen Bioinformatics Centre, University of Groningen) for helpful inputs and critical readings of this manuscript.

Figure 2.1: The egg-laying circuit activity in regards to egg-laying. (A) The anatomical connections of the egg-laying related neurons and muscles. (B) The combined visible and fluorescent microcopy catches both the cameleon signal and egg-laying events. Part of a hermaphrodite worm body was on the right bottom conner of the imag.e. The body border is indicated by a line; the vulva is indicated by a star; the HSN cell body is indicated by white arrows. One egg-laying event occurred during the third frame and is revealed by weak visible light. To better view the egg-laying events, the original pictures is adjusted in the contract as shown in the bottom row. (C) Egg-laying events are coupled with the neural activities in vm2, vm1, HSN and VC cells. The blue lines are time-lapse cameleon signals, the relative change in its YFP/CFP ratio, which also represents the relative intracellular calcium concentrations. Red lines indicate the times egg-laying events occurred. Scale bars for cameleon signals are as indicated.

A.

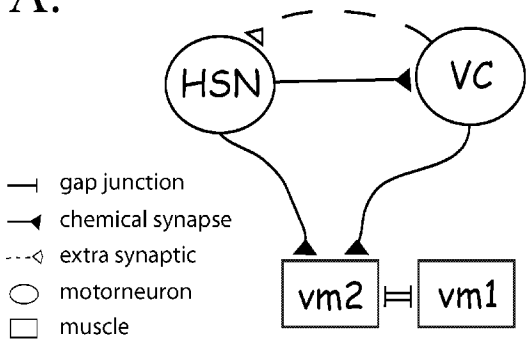

B.

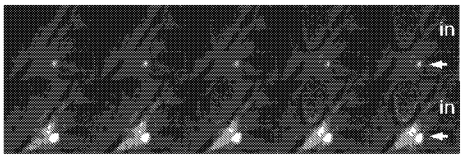

time : 100 200 300 400 500 ms

C.

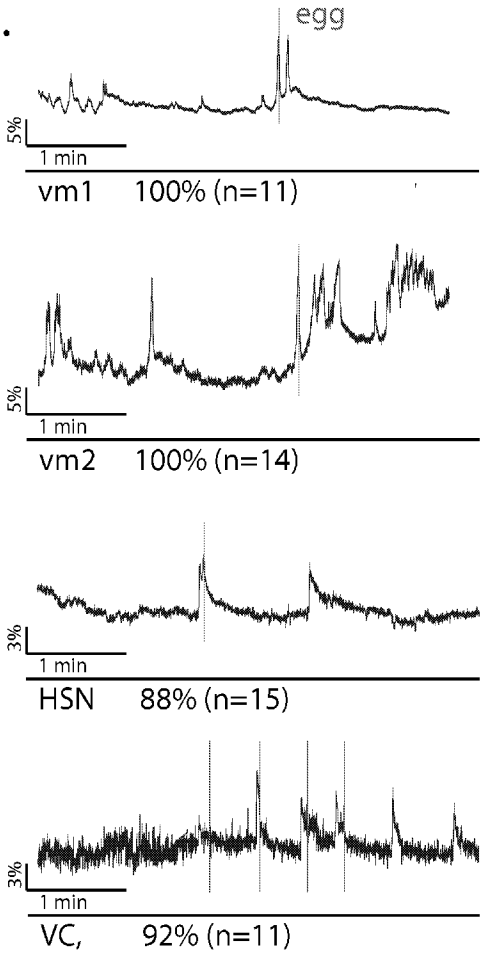

Figure 2.2: Osmolarity affects egg-laying behavior and neural activities. (A) Does response of egg-laying to different osmolarity buffers made from sucrose. Each blue dot represents one worms; the red circles indicate the mean of egg-laying event numbers; standard errors of means (SEM) are also shown as extended red lines. (B) Representative HSN and VC activities of wild type worms in extreme osmolarity conditions are revealed by cameleon signals. (C) The means and SEMs of spike frequencies are plotted to illustrate the HSN and VC responses to different osmolarities. (D) The HSN and VC responses to acute low osmotic shock. A low osmolarity inflow was opened at 30 seconds after recording begins. N represents the number of worms that showed similar responses as illustrated here. All blue traces are cameleon signals representing relative intracellular calcium concentrations. Scale bars are as indicated.

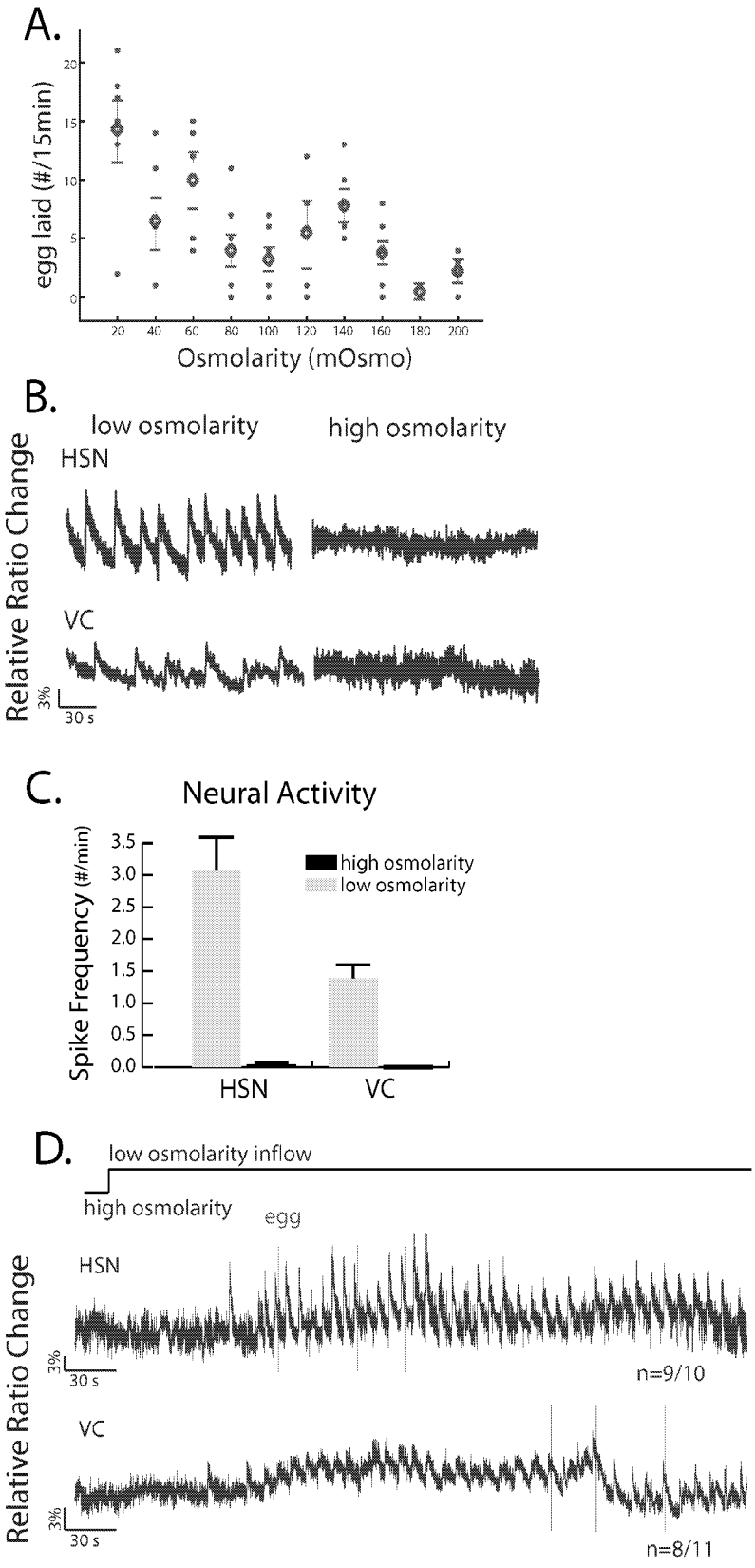
A.
egg laid (#/15min)
0
5
10
15
20
20 40 60 80 100 120 140 160 180 200
Osmolarity (mOsmo)
B.
low osmolarity
high osmolarity
HSN
VC
Relative Ratio Change
3%
30 s
C.
Neural Activity
Spike Frequency (#/min)
0.0 0.5 1.0 1.5 2.0 2.5 3.0 3.5
high osmolarity
low osmolarity
HSN
VC
D.
low osmolarity inflow
high osmolarity
egg
HSN
Relative Ratio Change
3%
30 s
n=9/10
VC
3%
30 s
n=8/11

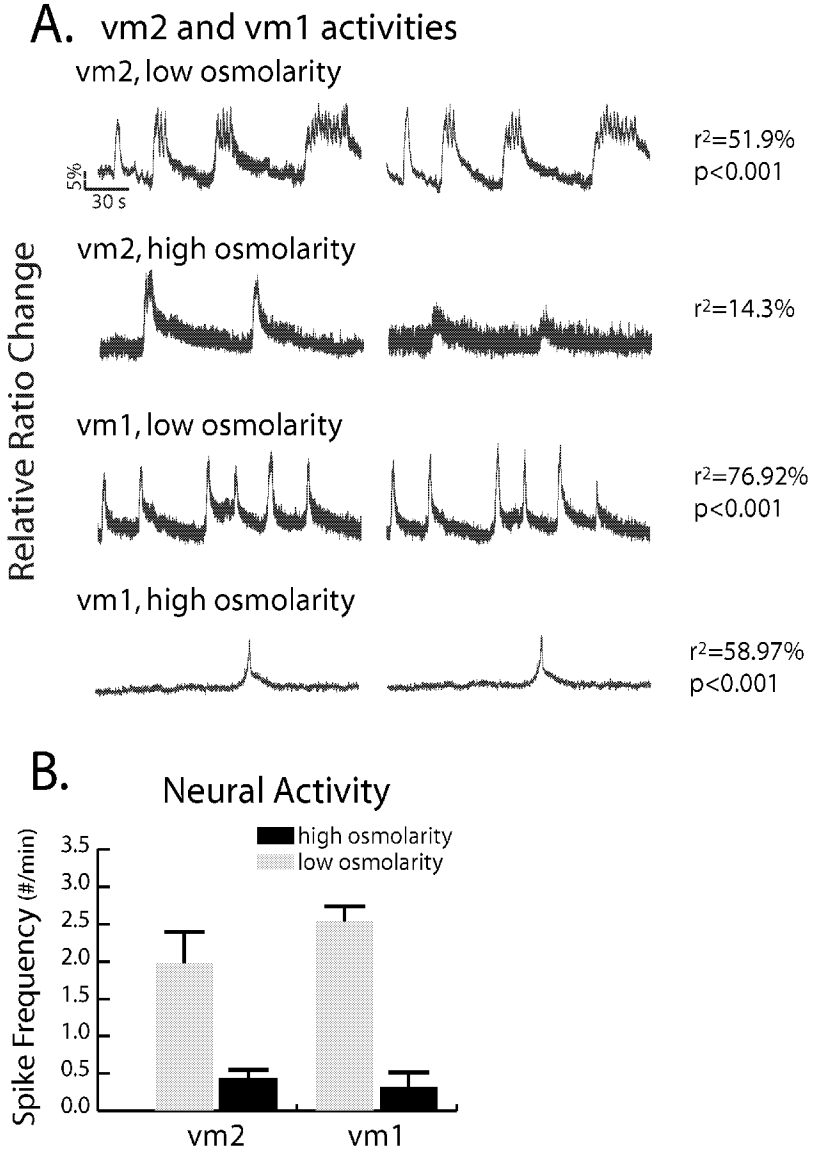

Figure 2.3: The vm2 and vm1 activities respond to different osmolarity conditions. (A) Two vm1 or vm2 cells are imaged simultaneously in each single worms and the cameleon traces are represented on the same lines. Scale bars are as indicated. r^2, the variation percentage, is calculated and indicated. The statistical p values are indicated if significant.

Figure 2.4: The interactions between the HSN and VC cells. (A) Both the HSN and VC activities are simultaneously captured with the help of a worm rotating device (Suzuki unpublished). The red trace is the HSN activity and blue ones are VC4 and VC5 activities. Dashed lines indicate the coupled activities. (B) Representative HSN and VC activities are changed due to the lack of the other cell type. (C) The means and SEMs of the spike frequencies are plotted to represent the HSN and VC activities in situations illustrated in (B). Scale bars are as indicated in the figure.

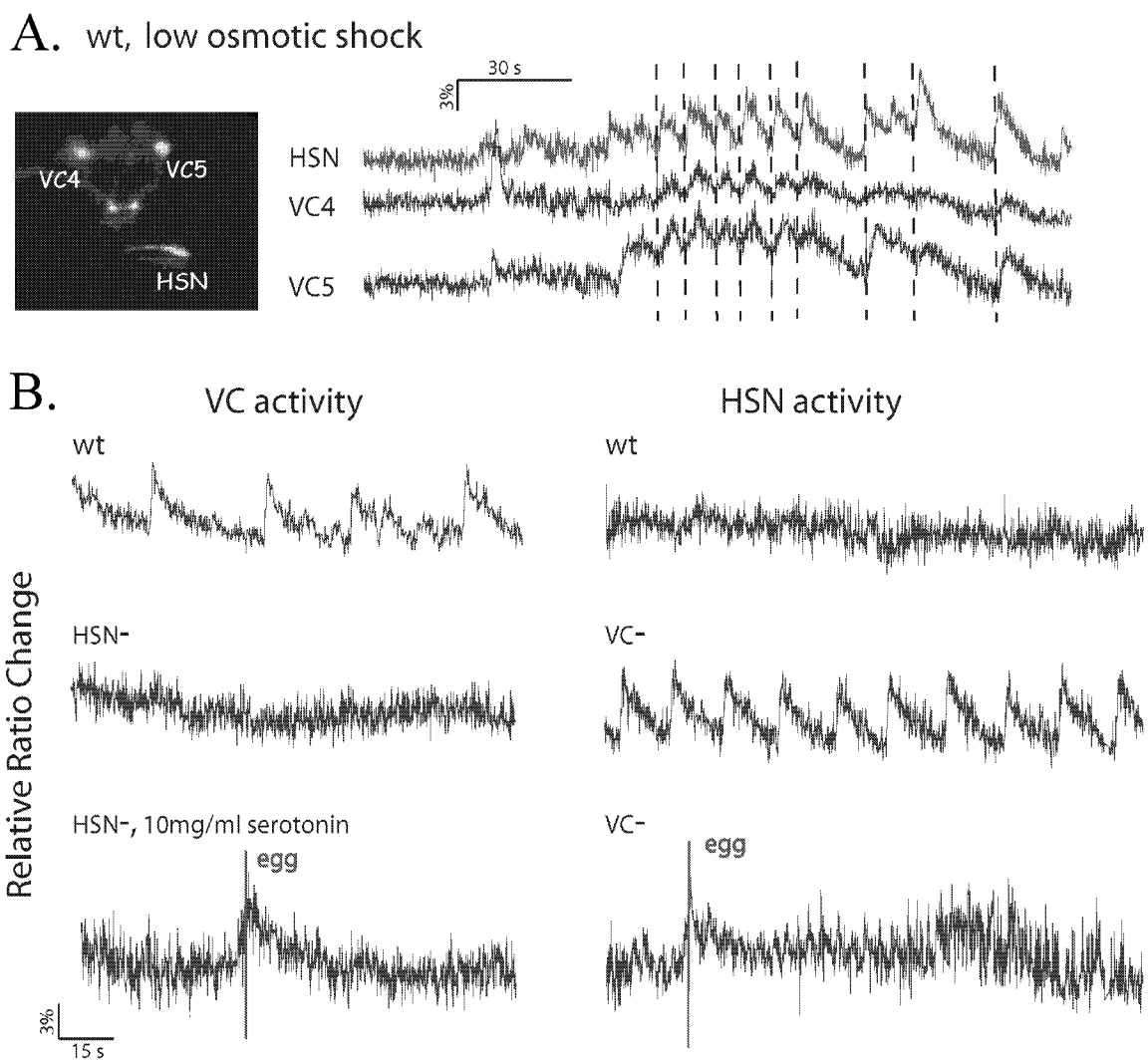
A.
wt, low osmotic shock
30 s
3%
VC4
VC5
HSN
HSN
VC4
VC5
B.
VC activity
HSN activity
wt
wt
HSN-
VC-
HSN-, 10mg/ml serotonin
VC-
egg
egg
Relative Ratio Change
3%
15 s
C.
Neural Activity
high osmolarity
low osmolarity
Spike Frequency (#/min)
3.0
2.5
2.0
1.5
1.0
0.5
0.0
HSN
VC
wt
VC-
wt
HSN-

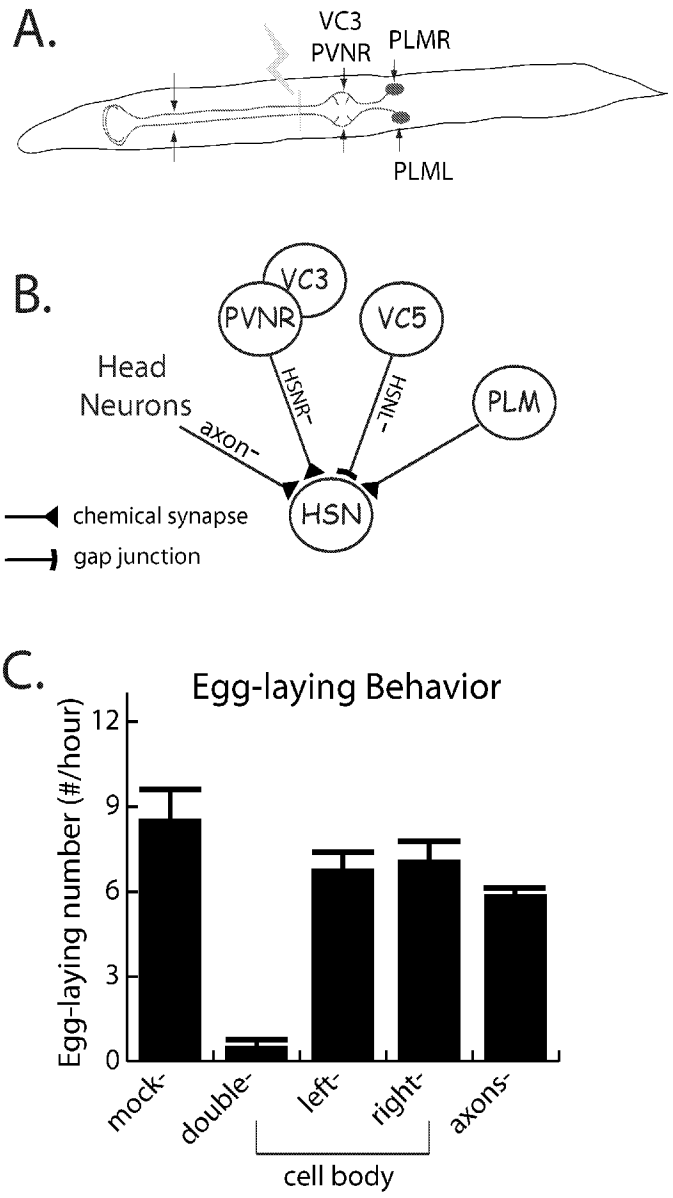

Figure 2.5: The HSN cell is independent of synaptic inputs to generate spike activities. (A) An illustration of synaptic input distributions on the HSN cell bodies and along their axons. The focuses of femtolaser microsurgery are indicated by the crosses between the yellow line and HSN axons. (B) A summary of all HSN synaptic inputs and their ablations in corresponding laser surgeries. (C) The results of the egg-laying behavior assays on laser operated worms as indicated.

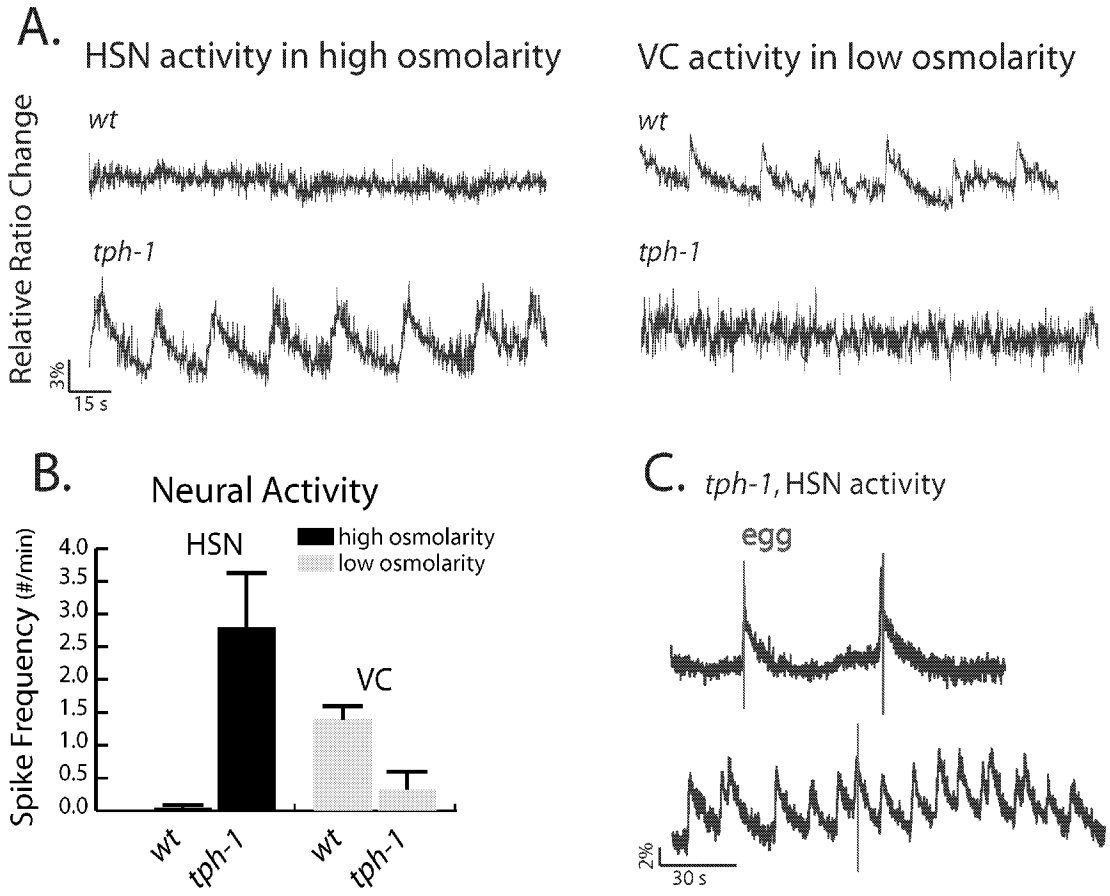

Figure 2.6: The HSN and VC activities in *tph-1(mg280)*, serotonin synthesis null, mutant worms. (A) Representative HSN and VC activities in *tph-1* mutant worms. (B) The means and SEMs of spike frequencies are plotted to represent the HSN and VC activities in *tph-1* worms. (C) The coupling of egg-laying events with the HSN activity in *tph-1* worms is shown. The blue lines are cameleon signals; the red vertical lines indicate the times egg-laying events occurred. Scale bars are as indicated.

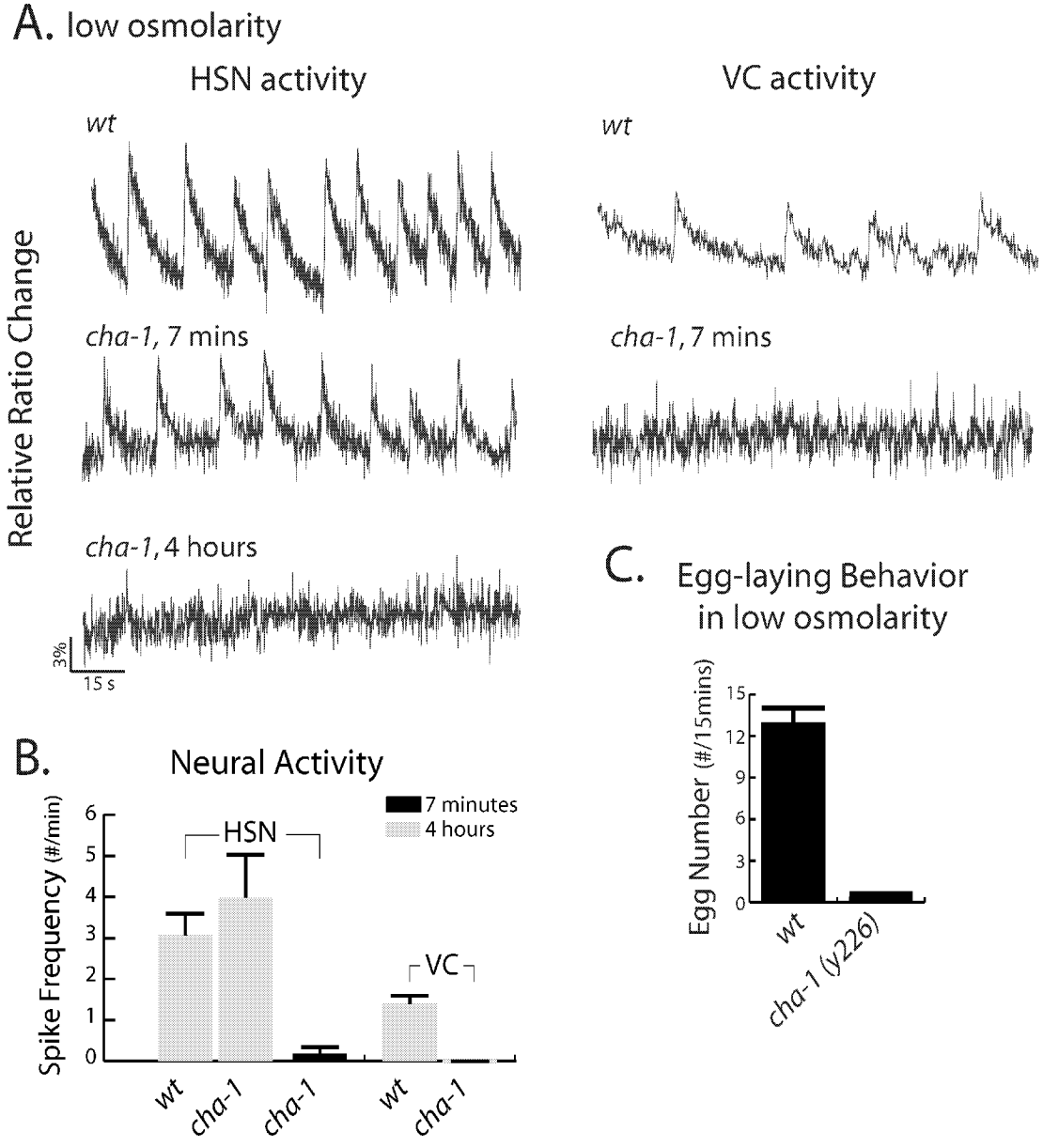

Figure 2.7: The HSN and VC activities in *cha-1(y226)*, an acetylcholine synthesis temperature sensitive allele, mutant animals. (B) Representative HSN and VC activities in *cha-1* mutant animals at the indicated timings after being moved to the restrictive temperatures are revealed by cameleon signals. (C) The means and SEMs of spike frequencies are plotted to represent the HSN and VC activities. (C) Results of the egg-laying behavioral assay performed on *cha-1* mutant animals.

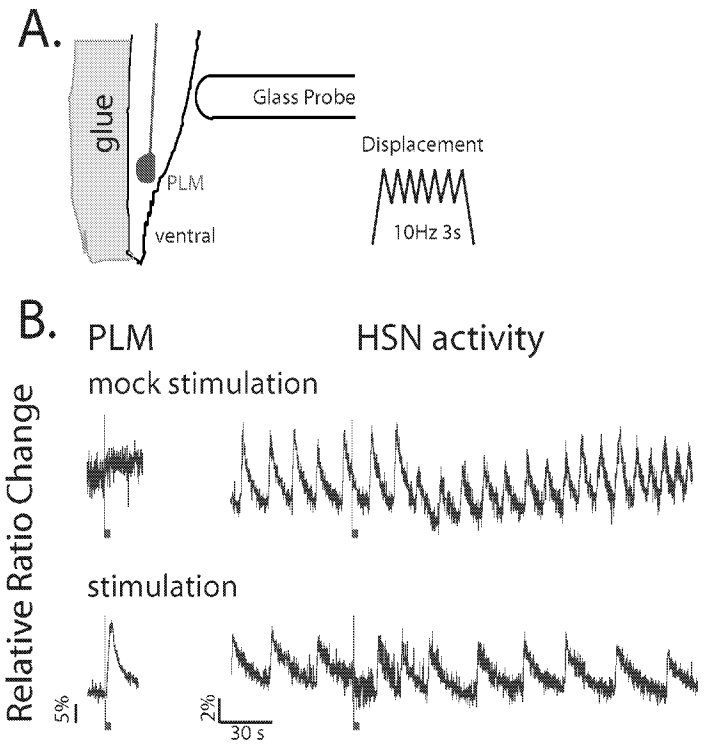

Figure 2.8: The PLM, posterior mechanoreceptor neuron, transiently inhibits HSN activity. (A) The mechanical stimulation and the setting to stimulate the PLM cell are illustrated. (B) Representative traces of PLM and HSN activities are shown. The red vertical bars indicate the beginning of the stimulations and the rectangulars at its bottom indicate the time period of the whole stimulations.

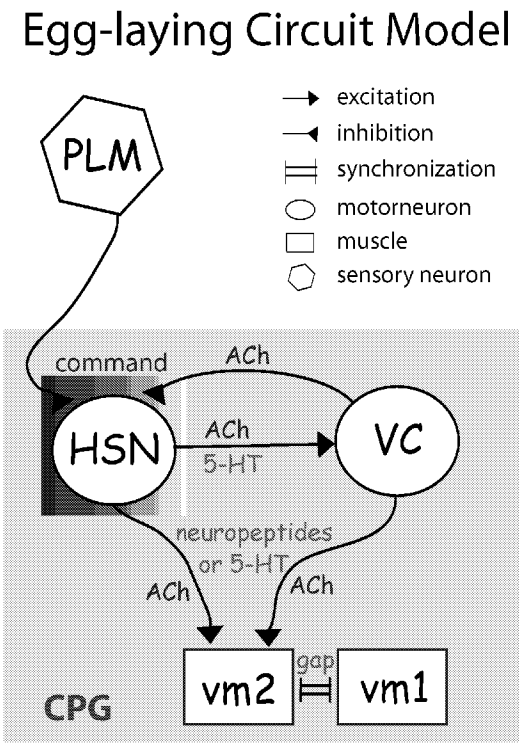

Figure 2.9: The model on the functionality of the egg-laying circuit based on our results and others that have been previously published. Figure legends are as illustrated. ACh and 5-HT stand for the neurotransmitters acetylcholine and serotonin repectively.

The text of Chapter II will be to be submitted to a peer review journal. The author list includes Mi Zhang, Samuel H. Chung, Caroline R. Craig, Hiroshi Suzuki, Rex Kerr, Eric Mazur and William R. Schafer. I am the primary author of this part of research. Samuel in Mazur's group performed all laser surgeries on the HSN cell body and axons. Hiroshi developed the worm rotating device employed in HSN and VC simultaneous imaging experiment. The idea of using combined visible and fluorescent microscopy is upon Rex's suggestion. Schafer, Callie and I finished text writing.

CHAPTER III. A VOLTAGE-GATED CATION CHANNEL-LIKE PROTEIN NCA-1 AND A NOVEL PROTEIN UNC-80 REGULATE SYNAPTIC ACTIVITY AND DEVELOPMENT IN *CAENORHABITIS ELEGANS*

ABSTRACT

Voltage-gated cation channels regulate neuron excitability through selective ion flux. NALCN, a member of a protein family structurally related to α1 subunits of voltage-gated sodium/calcium channels was recently shown to control the firing of mouse neurons through regulating resting membrane potentials. We identified a gain-of-function allele of NCA-1, a *C. elegans* member of this protein family. *nca-1* gain-of-function mutants display abnormal distributions of active zone markers, increased presynaptic calcium transients and exaggerated body bends in locomotion. Loss of NCA activities leads to calcium transient silencing at synapses without affecting calcium influx at cell bodies, reduced synaptic transmission at neuromuscular junctions and frequent halting in locomotion. NCA-1 localizes along axons, enriched at non-synaptic regions. Its localization and function depend on UNC-80, a novel conserved protein also enriched at non-synaptic regions. We propose that NCA-1 and UNC-80 regulate synaptic activity and morphology by propagating depolarization signals to synapses in *C. elegans* neurons.

INTRODUCTION

Neurons generate and propagate electrical signals along nerve processes, converting them into chemical communication through neurotransmitter release at

synapses. By allowing selective ion flux across the plasma membrane, cation channels regulate the excitation and function of neurons. In most nervous systems, action potentials, the traveling and rapidly reversing membrane potentials are induced by the opening of voltage-gated sodium channels and modulated by voltage-gated sodium, potassium and occasionally calcium Ca^{2+} channels(Hille, 2001; Llinas, 1988). Action potential-induced depolarization at presynaptic termini triggers the opening of voltage-gated calcium channels (VGCCs), leading to an influx of Ca^{2+} that allows for Ca^{2+} dependent synaptic vesicle exocytosis(Catterall, 1999).

Voltage-gated sodium channels consist a pore-forming $\alpha 1$ subunit and variable numbers of auxiliary β subunits(Yu and Catterall, 2003). They display similar properties and possess similar functions in establishing the threshold and generating action potentials. In contrast, multiple neuronal VGCCs differ in composition, property, localization and function. All known VGCCs are composed of a pore-forming $\alpha 1$ subunit, which associates with various accessory $\alpha 2\delta$, β and γ subunits that modulate the property of the channel(Catterall, 2000; Catterall et al., 2005; Yu and Catterall, 2003). Vertebrates have at least six families of VGCCs with different opening probability and kinetics(Catterall, 2000; Catterall et al., 2005; Yu and Catterall, 2003). Among them, P/Q- and N-type VGCCs are components of the active zone, the presynaptic subcellular structure where synaptic vesicles are released(Couteaux and Pecot-Dechavassine, 1970; Garner et al., 2000), and mediate the Ca^{2+} influx that triggers the membrane fusion between synaptic vesicles and presynaptic termini(Pietrobon, 2005). Other VGCCs can also participate in the modulation of neuronal excitation, affecting the duration of action potentials of specific neurons(Llinas, 1988; Yarom et al., 1985).

C. elegans does not encode voltage-gated sodium channel orthologues or display typical voltage-gated sodium currents(Franks et al., 2002; Goodman et al., 1998; Jospin et al., 2002; Richmond and Jorgensen, 1999; Shtonda and Avery, 2005; Vinogradova et al., 2006). Therefore *C. elegans* cells either do not generate action potentials, or generate and propagate atypical action potentials through alternative mechanisms such as VGCCs in muscles(Jospin et al., 2002; Shtonda and Avery, 2005; Steger et al., 2005). *C. elegans* neurons are proposed to possess membrane properties that may allow the passive spreading of electrical signals(Goodman et al., 1998). But the nature of excitation signals and how they are propagated in *C. elegans* neurons are unknown.

C. elegans encodes a single P/Q-, N- and R-family VGCC α1 subunit (UNC-2), one L-type α1 subunit (EGL-19) and one T-type α1 subunit (CCA-1)(Lee et al., 1997a; Schafer and Kenyon, 1995; Steger et al., 2005). UNC-2 is proposed to localize at presynaptic active zones and affect the neurotransmitter release(Mathews et al., 2003). The loss of UNC-2 function leads to slow and abnormal locomotion, failure in neuronal migration and abnormal sensitivity to dopamine and serotonin(Mathews et al., 2003; Schafer and Kenyon, 1995; Tam et al., 2000). In pharyngeal muscles, the excitability threshold is set by CCA-1, which initiates an atypical action potential in response to depolarization(Shtonda and Avery, 2005; Steger et al., 2005). EGL-19 generates Ca^{2+} transients that define sarcomere excitability(Jospin et al., 2002; Lee et al., 1997a; Shtonda and Avery, 2005). It also contributes to Ca^{2+} transients in cultured mechanosensory neuron cell bodies(Frokjaer-Jensen et al., 2006).

A rat cDNA clone encoding a novel protein with homology to the α1 subunit of voltage-gated cation channels was first isolated by degenerative oligo-based PCR

screening(Lee et al., 1999). Homologues of this protein are found in various animals, namely NCA-1 and NCA-2 in *C. elegans*(Humphrey et al., 2007), Dmα1U/CG1517 in *C. elegans*(Nash et al., 2002) and Vgcnl1/NALCN(Lu et al., 2007) in mouse, rat and human. This protein family displays divergence from known voltage-gated sodium/calcium channels in the key amino acids that control ion selectivity, as well as in structures responsible for voltage-sensitivity, suggesting that this new protein family may form channels with unique kinetics and composition. Indeed a recent paper showed that mouse NALCN alone forms a voltage-insensitive and poorly selective cation channel in HEK293 cells(Lu et al., 2007).

C. elegans Dmα1U mutants are viable but display altered sensitivity to anesthetics and abnormal locomotory circadian rhythm(Nash et al., 2002). Similarly, a *C. elegans nca-1;nca-2* double knockout mutant was recently shown to display abnormal halothane sensitivity and more frequent pause during locomotion (fainter)(Humphrey et al., 2007). The physiological basis for these defects, however, is unknown. *NALCN* knockout mice are neonatal lethal due to a disrupted respiratory rhythm(Lu et al., 2007). Mutant hippocampal neurons display reduced background Na^{2+} leak currents and less firing(Lu et al., 2007), suggesting that NALCN regulates neuronal excitability.

In a *C. elegans* genetic screen to identify genes affecting the development of presynaptic active zone(Yeh et al., 2005), we isolated a mutant *unc-77(hp102)* that displays an altered distribution of an active zone marker SYD-2::GFP. We demonstrate that *unc-77* mutants are gain-of-function alleles for *nca-1*. Our phenotypic analyses and expression studies of *nca* loss- and gain-of function mutations demonstrate a specific role of NCA proteins in regulating synaptic activity through propagating activation signals to

synapses. We further identify UNC-80, a unique auxiliary protein of the putative NCA channel. We propose that NCA/UNC-80 represents a novel channel complex that modulates the transduction of activation signals in *C. elegans* neurons.

RESULTS

hp102 mutants display abnormal synaptic active zone marker morphology

By tagging an active zone component SYD-2 with green fluorescent protein (GFP), we developed a marker *hpIs3* (*Punc*-25-SYD-2::GFP) that labels active zones of GABAergic neuromuscular junctions (NMJs) in live *C. elegans*(Yeh et al., 2005; Zhen and Jin, 1999). To uncover mechanisms that regulate active zone development and function, we performed a genetic screen that yielded several mutants with abnormal morphology and distribution of *hpIs3*, one of which is *hp102*(Yeh et al., 2005).

In wild-type larval stage (L2) animals, *hpIs3* fluorescent puncta distribute fairly evenly along the dorsal nerve cord (Figure 3.1a, *hpIs3* panel). In *hp102* mutants, they are clustered and interspersed by larger gaps (Figure 3.1a, *hp102* panel). Another active zone marker *hpIs61* that expresses a GFP-tagged active zone scaffolding protein UNC-10(Koushika et al., 2001) in GABAergic neurons shows similar changes. While wild-type animals display UNC-10::GFP puncta fairly uniform in size and distribution (Figure 3.1b, *hpIs61* panel), puncta become clustered in some areas, with gaps in other regions in *hp102* mutants (Figure 3.1b, *hp102* panel). Consistent with our qualitative observation, the quantified average distance between neighboring puncta in *hp102* animals was increased by 35% for *hpIs3* (1.□□±0.1□m for wild-type versus 2.29±0.3□m for *hp102*, p=0.048) (Figure 3.1d), and 47% for *hpIs61* (1.□□±0.1□m for wild-type versus

2.60±0.4□m for *hp102*, p=0.008) (Figure 3.1e), with a larger variability when compared to wild-type animals (Scatter plots in Supplementary Figure 3.1). Total *hpIs3* and *hpIs61* punctum numbers were reduced by 22.7% (36.7±2.2 for wild-type versus 27.0±2.4 for *hp102*, ~1/3 of the dorsal cord, p<0.0001) and 26.4% (139.4±7.0 for wild-type versus 107.7±9.5 for *hp102*, the entire dorsal cord, p<0.0001) respectively, suggesting a net loss of active zone components in *hp102* mutants (Figure 3.1d,e). In contrast, we observed no gross change in the distribution or morphology of *juIs1*, a vesicle marker (SNB-1::GFP) for GABAergic NMJs(Zhen and Jin, 1999) (Figure 3.1c, f), suggesting that *hp102* affects the development or function of active zones specifically. Using another active zone marker *hpIs54* that expresses GFP::SYD-2 by *Punc-129*, a promoter specific for cholinergic motoneurons(Colavita et al., 1998; Sieburth et al., 2005), we also observed frequent gaps in *hp102* mutants, which were rarely present in wild-type animals (Supplementary Figure 3.2). Therefore, *hp102* affects the distribution of active zone components in both GABAergic and cholinergic NMJs that regulate *C. elegans* locomotion. Consistently *hp102* mutants display locomotion abnormalities characterized by active but greatly exaggerated body bends (Supplementary Movie 1,2).

hp102 mutants also display hyperactived egg-laying behavior so that fewer and younger eggs remained in their uterus (Figure 3.1i,j). We then examined the synapse morphology of HSNs, the serotonergic neurons that innervate egg-laying vulval muscles as well as other motoneurons in the egg-laying circuit(Schafer, 2006). *wyIs12*, a marker that expresses GFP::SYD-2 in HSN shows distinct fluorescent puncta along the axon across the vulva ((Patel et al., 2006), Figure 3.1g). In *hp102* mutants, these puncta became more clustered and irregularly spaced along the axon (Figure 3.1g). Similar to

GABAergic NMJs, the vesicle marker for HSNs(Patel et al., 2006) showed no difference between wild-type and *hp102* animals (Figure 3.1h), suggesting a specific alteration in active zone components also at HSN synapses.

Our genetic mapping revealed that *hp102* is allelic to *unc(uncoordinated)-77(e625),* a mutant previously isolated based on its abnormal locomotion behavior ((Brenner, 1974), Method). *e625* mutants also display constitutive egg-laying(Schafer et al., 1996) as well as abnormal distribution of *hpIs3* similar to *hp102* mutants (not shown), corroborating that both mutations affect the same gene.

_hp102_ and _e625_ are gain-of-function alleles for _nca-1_

We mapped *hp102* (Methods) and identified a genomic fragment containing a single opening reading frame *C11D2.6* that restores the synapse morphology (Supplementary Figure 3.3), and locomotion defects of both *hp102* (Movie S3) and *e625* mutants (not shown). We further identified single missense mutations in *C11D2.6* in *hp102* and *e625* mutants (Figure 3.2a). *C11D2.6*, which was renamed as *nca-1* based on its predicted amino acid sequence(Mathews et al., 2003) encodes protein isoforms with homology to voltage-gated cation channel α1 subunits, and one of the two *C. elegans* members(Humphrey et al., 2007) of the newly defined NCA/Dm□1/Vgcn1/NaLCN family protein (Figure 3.2b). Unlike all known sodium and calcium channel $\square_1$-subunits, whose ion selectivity filter motifs are DEKA(Schlief et al., 1996) and EEEE(Sather and McCleskey, 2003; Yang et al., 1993), NCA proteins contain EEKE at corresponding positions.

Behaviorally both *hp102* and *e625* are semi-dominant alleles; heterozygous mutants display an intermediate locomotion pattern between wild-type and homozygous

mutants. Introduction of a *C11D2.6* genomic fragment harboring the *hp102* mutation into wild-type animals induced both behavioral (Supplementary Movie 4) and active zone marker (not shown) defects similar to those in *hp102* mutants. Thus, both *hp102* and *e625* mutations represent gain-of-function alleles of the *nca-1* gene. Defects in *hp102* and *e625* mutants are not affected by deletions in NCA-2, the other NCA protein that functions redundantly with NCA-1 ((Humphrey et al., 2007) and see below). Taken together these gain-of-function mutations, which may cause elevated or misregulated NCA activities, will be referred to as *nca(gf)* henceforth.

Loss-of-function mutations in NCA do not affect synaptic development

We further analyzed the function of NCA channels in synapse development by examining the synapse morphology in loss-of-function mutants. Deletion alleles for both NCA genes, *nca-1* (*gk9* and *tm1851*) and *nca-2* (*gk5*) were generated by *C. elegans* gene knockout services and analyzed. Neither displayed obvious defects in development, locomotion and synaptic marker morphology in various neurons (data not shown).

While *nca-1* and *nca-2* single deletion mutants are normal in locomotion, *nca-1;nca-2* double mutants display a locomotion deficit that was classified as fainter(Humphrey et al., 2007; Sedensky and Meneely, 1987). Fainters are capable of normal locomotion spontaneously or upon stimulation, but are unable to sustain continuous movement, succumbing to frequent and long periods of halting (Supplementary Movie 5). This synergistic fainter phenotype suggests that NCA-1 and NCA-2 function redundantly to control sustained activation of the locomotory system(Sedensky and Meneely, 1987). This synergism, together with our studies (see below) suggest that the phenotype of *nca-1;nca-2* double loss of function mutant

represent the physiological outcome in the complete absence of NCA-type channel function, and will be referred to as *nca(lf)* henceforth.

We analyzed the synapse phenotype of *nca(lf)* mutants. They display normal synaptic marker morphology (Figure 3.1a-f, *nca(lf)* panels), undistinguishable from either *nca-1* or *nca-2* deletion mutants alone, suggesting that while elevated or misregulated NCA activity affects active zone morphology, normal NCA channel activity is not required for synapse development.

NCA activity regulates presynaptic activation in HSN neurons

We next investigated how altered NCA affects neural activity. The genetically-encoded calcium sensor cameleon has been used in HSNs and other neurons as an indicator of neuronal excitation in intact *C. elegans*(Kerr et al., 2000). The large size of HSN synapses makes it possible to record Ca^{2+} transients in presynaptic regions as well as the cell bodies under conditions that constitutively activate egg-laying (Methods). In wild-type animals, most Ca^{2+} transients distribute as periodic trains of Ca^{2+}spikes (Figure 3.3a,b). The synaptic Ca^{2+} transients temporally correlated with transients in cell bodies, displaying similar spike frequency (2.6$\pm$0.8 spikes/minute at synapses versus 3.2$\pm$0.6 spikes/minute at cell bodies, $p>0.05$, Figure 3.3c, f) and similar time intervals between spikes in the trains (7.5$\pm$0.5 seconds at synapses versus 8.6$\pm$0.2 seconds at cell bodies, $P>0.05$, Figure 3.3d,g), suggesting that the neuronal excitation signals spread from cell bodies to presynaptic regions.

We then examined Ca^{2+} transients in *nca(lf)* mutants. In HSN cell bodies, we observed trains of Ca^{2+} spikes comparable to those in wild-type animals for spike frequency (3.5$\pm$0.6 spikes/minute for *nca(lf)* versus 3.2$\pm$0.6 spikes/minute for wild-type,

p>0.05), interval (5.8±0.2 seconds for *nca(lf)* versus 8.6±0.2 seconds for wild-type, p>0.05) and amplitude (5.3±0.6% for *nca(lf)* versus 6.9±0.4% for wild-type, p>0.05) (Figure 3.3C-H). In contrast, while synaptic Ca^{2+} transients were present in all wild-type animals, half of *nca(lf)* mutants showed no Ca^{2+} transients at all (Figure 3.3b *nca(lf)*, top trace). The rest of *nca(lf)* mutants displayed Ca^{2+} transient trains (Figure 3.3b, *nca(lf),* bottom trace). This resulted in an overall statistically significant decrease of synaptic spike frequency (1.2±0.7 spike/minute in *nca(lf)*) compared to wild-type synapse (2.6±0.8 spike/minute, p=0.029), or to *nca(lf)* cell bodies (3.5±0.6 spike/minute, p=0.005). Remarkably, the remaining trains of Ca^{2+} transients in *nca(lf)* mutants remained temporally correlated in spike interval (5.2±0.4 second) with the cell body of *nca(lf)* mutants (5.8±0.2 second, p>0.05). They also display comparable size (6.8±0.7%) to those in wild-type synapses (5.2±0.7%, p>0.05) (Figure 3.3c-h). Thus, the loss of NCA function specifically affects the initiation of Ca^{2+} transients at the HSN synapses.

In *nca(gf)* mutants, HSN neuron cell bodies displayed trains of calcium spikes similar to those in wild-type animals for spike frequency (3.3±1.0 spikes/minute for *nca(gf)* versus 3.2±0.6 spikes/minute for wild-type, p>0.05), spike interval (5.3±0.3 seconds for *nca(gf)* versus 8.6±0.2 seconds for wild-type, p>0.05) and spike size (9.2±1.4% for *nca(gf)* versus 6.9±0.4% for wild-type, p>0.05) (Figure 3.3a, c-e). At HSN synapses, all *nca(gf)* animals displayed trains of Ca^{2+} spikes that temporally correlated in frequency (2.7±0.8 spikes/minute) with those in *nca(gf)* cell bodies (3.3±1.0 spikes/minute, p>0.05), and in interval (6.4±0.3 seconds for synapses versus 5.3±0.3 seconds for cell bodies, p>0.05). However, the synaptic peak size was significantly increased in *nca(gf)* mutants (9.5±1.3% for *nca(gf)* versus 5.2±0.7% for wild-type,

p=0.029). Although the mean size appears only moderately bigger than in wild-type animals, *nca(gf)* animals exhibited a fraction of unusually large synaptic Ca^{2+} transients that were well above the range seen in wild-type animals (Figure 3.3h, red box).

In summary, since all recorded *nca(lf)* and *nca(gf)* animals had active Ca^{2+} transients at neuron cell bodies that were similar to wild-type animals, the displayed changes in their synaptic calcium influx suggest that under the assay conditions, NCA channel activity does not affect the excitation at HSN cell bodies. Since the loss of NCA activity leads to a decrease of Ca^{2+} influx and less presynaptic activity, and gain-of-function in NCA causes elevated Ca^{2+} influx that correlates with enhanced presynaptic activation, we hypothesize that NCA activity is important for conducting cell body activation signals to synapses.

NCA activity is required for synaptic transmission at NMJs

Calcium imaging at cholinergic and GABAergic NMJs is currently difficult due to the small synapse size. We therefore recorded spontaneous and evoked postsynaptic currents in body wall muscles as an indirect measure for presynaptic activity at *C. elegans* NMJs. In the presence of both low and high concentration of extracellular calcium, the *nca(lf)* mutants displayed a significant decrease in the frequency of spontaneous release (mPSP) (29.4±5.3 Hz, $p<0.01$ at 5mM Ca^{2+} and 11.8±2.5 Hz, $p<0.001$ at 1mM Ca^{2+}) compared to wild-type animals (55.6±5.3 Hz at 5mM $Ca^{2+}$and 39.7±6.5 Hz at 1mM Ca^{2+}) (Figure 3.4a). *nca(lf)* mutants also display significantly reduced evoked responses. Electric stimulation of the ventral nerve cord elicited currents (ePSP) of 1234.1±57.7pA in amplitude at 5mM Ca^{2+}, and 1080±161.3 pA at 1mM Ca^{2+} (Figure 3.4b). In *nca(lf)* mutants, the amplitude of evoked response was reduced by

about 60% at 5mM Ca^{2+} (523.9±57.7 pA, $p<0.001$), and about 75% at 1mM Ca^{2+} (278.6+109.2 pA, $p=0.01$) (Figure 3.4b). The reduced mPSP frequency as well as reduced ePSP amplitudes in *nca(lf)* mutants suggest a significant reduction of synaptic transmission at NMJs. The reduced synaptic transmission is consistent with the reduced locomotion activity in *nca(lf)* mutants and also reduced presynaptic activity at HSN synapses.

We also recorded from *nca(gf)* mutants, however this analysis appears unsuitable to examine the physiological status of motoneuron activity in these mutants. For undetermined reasons, no ePSP could be evoked in any dissected preparations even when they displayed normal mPSP. We also observed in these mutants acute resistance to levamisole, an agonist to acetylcholine receptors at NMJs, suggesting a potential modification at their postsynaptic machineries.

NCA-1 is expressed along axons but excluded from synapses

NCA may specifically regulate presynaptic activation by regulating either the local activation of synapses or the propagation of activation signals along axons. To investigate these possibilities, we examined the expression pattern of NCA-1. Promoter fusion constructs containing *nca-1* upstream genomic sequence revealed exclusive expression throughout the nervous system, including many sensory neurons, all GABAergic and cholinergic motoneurons and HSN neurons (Figure 3.4c). NCA-1 is indeed required in neurons since pan-neuronal expression of NCA-1 rescued the fainter defect of *nca(lf)* animals (Supplementary Movie 6). Furthermore, expression of NCA-1 by a GABAergic promoter *Punc-25*(Jin et al., 1999) rescued the *hpIs3* morphology

defects in *nca(gf)* mutants (Supplementary Figure 3.3), suggesting that NCA-1 functions cell-autonomously in neurons.

We generated an NCA-1 specific antibody that revealed dense and punctate staining in the nerve ring, a synapse rich region at CNS, and along the nerve cords that are comprised of inter- and motoneuron processes (Figure 3.4d, upper panel). These staining signals disappeared in *nca-1* deletion mutants (Figure 3.4d, lower panel). This specific and punctate staining pattern suggests subcellular enrichment along axons. We further examined the localization of NCA-1 relative to presynaptic termini using antibodies against vesicle protein SNB-1, the active zone protein UNC-10 and the presynaptic kinase SAD-1. We focused our analyses along the dorsal nerve cord where synapses are spatially separated. We observed non-colocalizing staining patterns between NCA-1 and all presynaptic proteins (Figure 3.4e, Supplementary Figure 3.4a), suggesting that NCA-1 is enriched at specific regions along motoneuron axons but not at synapses. This expression pattern is more consistent with NCA conducting activation signal propagation from neuronal cell bodies, rather than mediating Ca influx at synapses.

NCA-1 function is dependent on UNC-80

To define genes that regulate NCA activities, we performed a suppressor screen for the locomotion defects of *nca(gf)* mutants. One identified suppressor *hp369* failed to complement *unc-80*, an uncloned mutant first isolated by its locomotion defects ((Brenner, 1974), Supplementary Movie 7) and later shown to be hypersensitivity to halothane(Sedensky and Meneely, 1987). Previously isolated *unc-80* alleles also suppress the behavioral defects of all *nca(gf)* mutants (not shown).

unc-80 single mutants exhibit a fainter phenotype characteristic of *nca(lf)* mutants (Supplementary Movie 7). *nca(gf);unc-80* double mutants display the same fainter phenotype as *unc-80* mutants (Supplementary Movie 8). Furthermore, the active zone abnormality in *nca-1(gf)* mutants are rescued in *nca(gf);unc-80* double mutants (Figure 3.5a,b,d,e): the number of *hpIs3* and *hpIs61* puncta was restored from 27±0.7 to 37.5±1.2, and from 107.7±2.4 to 138.7±2.1, $p<0.001$, respectively. Taken together, *unc-80* is genetically epistatic to *nca(gf)* alleles.

Similar to *nca(lf)*, *unc-80* mutants display no gross defects in synaptic marker expression (Figure 3.5a-c). In addition, *nca(lf);unc-80* animals are indistinguishable from either *nca(lf)* or *unc-80* mutants alone in behavior (Supplementary Movie 9), suggesting that NCA and UNC-80 function in the same genetic pathway, and that NCA activity depends on UNC-80.

UNC-80 regulates synaptic activation in an identical fashion as NCA in HSN neurons

We further examined the effect of *unc-80* mutations on Ca^{2+} transients in HSN neurons using the cameleon Ca^{2+} sensor. As with *nca(lf)* mutants, in HSN cell bodies of all *unc-80* animals, we detected trains of Ca^{2+} transients with normal spike frequency (5.1±1.3 spikes/minute for *unc-80* versus 3.2±0.6 spikes/minute for wild-type, $p>0.05$), interval (5.8±0.2 second for *unc-80* versus 8.6±0.2 second for wild-type, $p>0.05$) and size (7.7±0.7% for *unc-80* versus 6.9±0.4% for wild-type, $p>0.05$) (Figure 3.3a, c-e). Likewise, half of these mutant animals showed complete silencing of Ca^{2+} transients at HSN synapses (Figure 3.3b, *unc-80*, top trace), and the other half displayed trains of Ca^{2+} transients, reducing the overall spike frequency (0.9±0.7 spikes/minute) when compared

to *unc-80* cell body (5.1±1.3 spike/minute, p=0.037), and wild-type synapses (2.6±0.8 spike/minute, p=0.032). The trains of Ca^{2+} transients in *unc-80* mutants contained Ca^{2+} spikes that remained temporally correlated with cell body transients in spike interval (5.6±0.5 seconds for synapses versus 5.8+0.2 seconds for cell bodies, p>0.05), and were comparable in size with wild-type synaptic transients (4.9±0.5% versus 5.2±0.7% for wild-type, p>0.05) (Figure 3.3b, *unc-80*, bottom trace, Figure 3.3c-e). Thus, the Ca^{2+} dynamics of *unc-80* mutants were essentially identical to those observed in *nca(lf)*, consistent with NCA and UNC-80 regulating the same aspect of HSN synaptic function.

UNC-80 encodes a novel protein that is expressed in neurons

We mapped *unc-80* mutations to a 1.8cM region on chromosome V (Methods). *unc-80* was determined to correspond to *F25C8.3* by Kim Schuske (University of Utah) based on the observation that RNAi knock-down of this open reading frame in wild-type animals resulted in a fainter phenotype (personal communication). We confirmed that genomic fragments containing only *F25C8.3* rescued the fainter phenotype of *unc-80* mutants (Supplementary Movie 8), and reverted *unc-80(e1272);nca(gf)* mutants from fainters to *nca(gf)* locomotion patterns (Supplementary Movie 11). *unc-80* encodes a large protein containing no known protein motifs, with uncharacterized homologues in *C. elegans*, mouse, rat and human (Figure 3.6), suggesting that it is a member of a novel but conserved protein family. We identified nonsense or splice junction mutations in three *unc-80* alleles, *e1272, hp369,* and *e1069* that are predicted to result in the loss of protein functions (Figure 3.6a). These alleles display phenotypes with a similar severity and penetrance, and similar genetic interactions with *nca(lf)* and *nca(gf)* mutants (not shown).

To determine where UNC-80 is expressed, we fused the predicted promoter sequence from the minimal rescuing genomic fragments with a GFP reporter. This reporter construct showed GFP expression throughout the nervous system, including most sensory neurons, all GABAergic and cholinergic motoneurons and HSN neurons, and in addition, in vulval muscles (Figure 3.7a). The neuronal expression pattern is similar to that of NCA-1, consistent with UNC-80 functioning in the same pathway as NCA.

UNC-80 and NCA-1 localize along nerve processes in a mutually dependent manner

We further examined the subcellular localization of UNC-80 using a functional P*unc-80*-UNC-80::RFP construct that rescued the fainter phenotype to the same degree as untagged genomic *unc-80* (Method, Supplementary Movie 12). We examined UNC-80 subcellular localization by staining *unc-80* mutants carrying *hpIs98*, an integrated transgenic array of P*unc-80*-UNC-80::RFP, with antibodies against RFP. We observed specific and punctate staining at the nerve ring and along nerve processes (Figure 3.7b-c, wild-type animals as negative controls). These staining signals do not co-localize with synaptic proteins (Figure 3.7c, Supplementary Figure 3.4b). The UNC-80::RFP staining pattern is highly reminiscent to that displayed by NCA-1, suggesting that UNC-80 proteins are also enriched at non-synaptic regions along nerve processes. Together with the fact that UNC-80::RFP signals were not observed in neuronal cell bodies (not shown), UNC-80 also regulates synaptic activation along axons.

To determine the functional relationship between UNC-80 and NCA-1, we examined the distribution of NCA-1 in *unc-80* mutants, and vice versa. While wild-type animals showed discrete NCA-1 staining at the nerve ring and along nerve cords, NCA-1

staining was completely or greatly diminished in multiple *unc-80* alleles (Figure 3.7d, *unc-80* panel). *hpIs98* (P*unc-80*-UNC-80::RFP) restored NCA-1 expression at the nerve ring and along the nerve cords in *unc-80* mutants (Supplementary Figure 3.5a). Also, while abundant NCA-1 staining was present in *nca(gf)* mutants, the staining was diminished in *nca(gf);unc-80* mutants (Figure 3.7d). Therefore, both wild-type and gain-of-function NCA-1 proteins depend on UNC-80 for their localization and/or stabilization along nerve processes. *nca-1* transcripts were present at similar levels between *unc-80* mutant and wild-type animals (Supplementary Figure 3.5b), supporting that UNC-80 regulates NCA-1 at the post-transcriptional level.

Interestingly UNC-80::RFP staining in the nerve ring and along nerve processes was also dramatically reduced in *nca(lf)* mutants (Figure 3.7b, *nca(lf);hpIs98* panel), suggesting that UNC-80 localization along the axon is dependent on the presence of NCA protein. UNC-80::RFP-dependent localization of NCA-1, and the fact that no transmembrane motifs are present in UNC-80, suggest that UNC-80 functions as an auxiliary component to stabilize, and may also regulate NCA function at the membrane.

DISCUSSION

In a genetic screen for regulators of active zone development, we isolated a gain-of-function mutation in a cation channel-like protein NCA-1. We reveal that the activity of NCA-1, regulated by a novel protein UNC-80, modulates synapse activation and composition. *nca(gf)* mutants display an abnormal distribution of active zone markers in several neurons, unaltered Ca^{2+} transients in cell bodies but increased transient amplitudes at synapses. In contrast, both *nca(lf)* and *unc-80* mutants display silencing of

synaptic Ca^{2+} transients without affecting Ca^{2+} transients at cell bodies. NCA-1 and UNC-80 are enriched at non-synaptic regions along nerve processes in a mutually dependent fashion. We propose that (Figure 3.8): 1) a NCA/UNC-80 complex propagates and/or modulates some activation signals from the cell body along the axon, 2) active zone development is influenced by, and/or re-enforces changes in synaptic activation.

NCA and UNC-80 transmit activation signals in neurons

In wild-type HSN neurons, the frequency and interval between calcium spikes at cell bodies and synapses are similar, suggesting temporally correlated activation. Upon stimulation, mutations in NCA did not alter Ca^{2+} transients at cell bodies, but in some *nca(lf)* and *unc-80* mutants, synaptic Ca^{2+} transients were silent, and in *nca(gf)* mutants, the presynaptic Ca^{2+} transients are increased in size, suggesting that NCA activity positively regulates presynaptic activation. The reduction of postsynaptic currents in *nca(lf)* mutants confirms that NCA activity is required for synaptic transmission at NMJs. Together with their non-synaptic localization along nerve processes, we propose NCA-1 and UNC-80 control synaptic activity through propagating neuronal excitation to synapses in *C. elegans* neurons.

The mouse NALCN mediates the background Na^{+} leak current that affects the resting potential and controls the excitability/firing rate of hippocampal neurons(Lu et al., 2007). Our studies reveal NCA propagates the activation signal to synapses, but do not rule out the possibility that NCA also controls neuronal firing. Our calcium imaging analysis was performed under conditions that stimulated the constitutive firing of HSNs, therefore an altered firing ability may be masked by the hyperactivation of neurons.

Strong stimulation was not sufficient to rescue the neurotransmission defects at *nca(lf)* NMJs, supporting a role of NCA in propagating excitation signals, but the reduction of evoked responses may still result from a combination of decreased firing and propagation. Some indirect evidence supports that NCA may also modulate neuronal firing: in solutions that inhibited calcium transients in HSN neurons of wild-type animals, some calcium transients persisted in *hp102* mutants (our unpublished observation). The ability of HSNs in *hp102* mutants to fire under inhibitory conditions suggests that *nca(gf)* mutations increase neuronal excitability, and that altered NCA activity affects neuron firing under different conditions.

Regardless of its potential implication in neuronal firing, the role of NCA and UNC-80 in activity propagation is important for neurons. The typical form of neuronal excitation and propagation is voltage-gated sodium channel-mediated action potentials, which are not present in *C. elegans*(Franks et al., 2002; Goodman et al., 1998; Jospin et al., 2002; Richmond and Jorgensen, 1999; Shtonda and Avery, 2005; Vinogradova et al., 2006). In *C. elegans* sensory neurons, current injections induced graded depolarizing signals(Goodman et al., 1998), which may play equivalent roles as action potentials. Yet how excitation signals reach synapses is unknown. The homology of NCA with NALCN, and its expression pattern make it a promising candidate as a modulator of activity propagation. One plausible model is that by regulating membrane potential (e.g. cation leak) at specific regions along nerve processes, NCA/UNC-80 channel participates in the propagation of membrane excitation along the axon. This model is also consistent with the increased Ca^{2+} transients in *nca(gf)* mutants where a hyperactivated NCA

channel along the axon may lead to enhanced depolarizing signals when they reach synapses.

NCA and UNC-80 selectively transmit signals from neuronal cell bodies

The complete silencing of HSN synaptic Ca^{2+} transients was observed in only half of the *nca(lf)* or *unc-80* mutant populations. The simplest explanation for this partial penetrance is that this represents a partial loss-of-function phenotype. This is unlikely since all *nca(lf)* and *unc-80* alleles used in this study are behaviorally indistinguishable from each other, and 100% penetrance in the fainter phenotype, which strongly argues against allelic effects on the penetrance of synapse activation defects. Moreover, *gk9* and *gk5* alleles delete essential pore-forming domains of NCA proteins, and the mutation in *unc-80(hp369)* leads to a relatively early stop codon, all implying a severe disruption of the protein function. Thus, *nca(lf)* and *unc-80* mutant phenotypes likely represent the physiological outcome of a complete loss of NCA activity.

We think the partial penetrance in Ca^{2+} transient loss likely represents that while some excitation signals from HSN cell bodies depend on NCA/UNC-80 to reach presynaptic termini, and some signals do not. Depending on the property of NCA/UNC-80, it is conceivable that the membrane potential changes it induces interfere only with the propagation of depolarization signals of certain amplitudes. In free-moving animals, HSN neurons integrate complex sensory inputs and innervate multiple postsynaptic cells(White, 1986). It is reasonable for them to fire activation signals of different intensities in response to different inputs. During locomotion, every animal alternates between a state of movement and quiescence. Extrapolating from calcium imaging analysis in HSN neurons, neurons in motor circuits may also fire alternative electrical

signals that are dependent or independent of NCA/UNC-80 to induce presynaptic activity to contribute to the switch between active and quiescent states. This may also explain our electrophysiology analysis on NMJs of *nca(lf)* mutants, where the dissected preparations displayed spontaneous postsynaptic currents ranging from wild-type-looking pattern to any currents at all.

NCA indirectly affects active zone development

We observed no obvious changes in active zone or vesicle markers in *nca(lf)* and *unc-80* mutants, indicating that NCA activity is not essential for establishing synaptic structures. In *nca(gf)* mutants, on the other hand, active zone markers show abnormal distributions in multiple neurons, suggesting that hyper- or mis-regulated NCA activity modifies synaptic composition. Abnormal morphology of active zone components at HSN synapses may parallel the observed increase of presynaptic activition at HSN synapses. The decrease in the total active zone punctum number in GABAergic synapses may result from a compensation for the increased excitation of other synapses in the same neural circuit.

Feedback regulation between synaptic activity and differentiation has been observed in multiple nervous systems. At *C. elegans* NMJs homeostatic signaling between synaptic strength and growth is well documented(Coyle et al., 2004). Prolonged synaptic inactivation by disrupting synaptic VGCCs also leads to the disintegration of active zones at mouse NMJs(Nishimune et al., 2004). Interestingly in *nca(gf)* mutants, the observed change is specific for active zone components, suggesting that active zones can be specifically altered in response to changes in synaptic excitation. Changes in

synaptic activation may even be re-enforced by the dynamic recruitment of active zone components to synapses as a homeostasis mechanism.

Unique properties of NCA/UNC-80 channel complexes

Despite of the shared sequence homology and predicted topology, NCA family proteins display distinctive properties from related pore-forming α1 subunits of voltage-gated sodium channels and VGCCs. Consistent with its difference in key positions for ion selectivity, in HEK293 cells mouse NALCN forms a non-selective cation channel. This channel is also insensitive to voltage, which is attributed to a reduction of charged amino acids in the voltage-sensing fourth transmembrane domains(Lu et al., 2007).

Cation channels are also distinguished by their auxiliary subunits. UNC-80 is a unique and exclusively required component of NCA mediated function. Not only do *unc-80* mutants show identical phenotypes as *nca(lf)* mutants and fail to enhance *nca(lf)* mutants, they suppress the behavior and active zone differentiation defects exhibited by *nca(gf)* mutant. By contrast, *unc-80* mutants do not phenocopy any VGCC mutants (Supplemental Table 1, Movie S13). Genetic interactions between *unc-80* and VGCC mutants, in particular, the lack of suppression of phenotypes induced by gain-of-function mutations in L-type VGCC, strongly suggest that UNC-80 is not a shared subunit for VGCCs (Supplemental Table 1). In fact, the mostly additive genetic interactions displayed between *unc-80/nca* and VGCC mutants (Supplemental Table 1) are more consistent with these two types of channels regulating different aspects of neuronal excitation.

An intriguing property of the putative NCA/UNC-80 channel complex is that NCA-1 and UNC-80 depend on each other for membrane localization. Therefore UNC-

80 may also modulate NCA channel activity after trafficking or stabilizing NCA along the axon. It has been recently reported that the protein level of NCA family proteins is reduced in *Dunc-79/unc-79* mutants in *C. elegans* and *C. elegans*(Humphrey et al., 2007). UNC-79 is a novel protein whose tissue specificity and subcellular localization are unknown(Humphrey et al., 2007). *unc-79* mutants are also fainters, suggesting it may represent another unique component of the NCA channel.

METHODS AND MATERIALS

Strains

All strains were cultured at 22°C unless specified otherwise. *hp102* was originally identified in a genetic screen for *hpIs3* defective mutants(Yeh et al., 2005) and outcrossed 8 times against wild-type N2. *unc-80(hp369)* was identified in a *hp102* suppressor screen and outcrossed 3 times against N2. *e625*, *e1069* and *e1272* were identified through abnormal locomotion in previous *C. elegans* screens(Brenner, 1974). *gk9* and *gk5* were generated by the Gene Knockout Consortium and outcrossed 3 times against N2. *tm1591* was generated by National Bioresource Project for the Nematode and outcrossed once against *N2*.

Immunocytochemistry

An antibody against aa1731-1914 of the predicted NCA-1d isoform was generated in rat (*Covance*). Whole-mount immunofluorescent staining was carried out as previously described(Hung et al., 2007). Antibodies against NCA-1, mRFP (*Clontech*), SAD-1, SNB-1 and UNC-10 (M. Nonet, Washington University, St. Louis) were used in 1:10, 1:200, 1:200, 1:100 and 1:2000 dilutions, respectively.

Calcium imaging

Pcat-1-cameleon was used to reveal relative Ca^{2+} concentrations in HSN cell bodies and synapses corresponding those on vm5 muscles. Adults 24 hour post L4 stage were immobilized by surgical glue on 2% agarose pads on microscope slides and covered with 1ml 10mM HEPES (pH 7.1). Recording was carried out as previously described(Kerr, 2006). All recordings started within 2 minutes after animals were glued and lasted for 10 minutes. Data from HSN cell bodies and synapses were obtained simultaneously. Due to slight body movements during the recordings, some synapse data sets were incomplete and were not included in analysis. Spike detection, data analysis and statistic analysis by Kolmogorov-Smirnov rank test due to abnormal data distribution were carried out as described previously ((Shyn et al., 2003) and Supplemental).

Imaging and quantification of synaptic markers

Imaging of synaptic markers was performed as previously described(Yeh et al., 2005). A MATLAB script was used for quantitative analyses as described ((Hung et al., 2007) and Supplementary Figure 3.1).

Electrophysiology

Dissections on young adult *C. elegans* were performed as described(Jospin et al., 2002; Richmond and Jorgensen, 1999). The integrity of the anterior ventral medial body muscle and the ventral nerve cord was visually examined and muscle cells were then patched using fire-polished 4MegaOhms resistant borosilicate pipettes (*World Precision Instruments*), clamped at -60mV using a Axopatch 1D amplifier throughout experiments (*Molecular Devices*), and recorded using the whole-cell patch-clamp technique in previously described recording solutions(Touroutine et al., 2005) within 5 minutes

following the dissection. Signals were filtered at 5kHz, and digitized via a Digidata 1322A acquisition card (*Molecular Devices*), and data were acquired and analysed using the pClamp software (*Molecular Devices*). After 10-60s of recoding of spontaneous events, a highly resistant fire-polished electrode filled with 3M KCl was brought close to the ventral nerve cord region anterior to the recorded muscle cell, and a 1ms depolarizing current was applied to induce an evoke response.

ACKNOWLEDGEMENT

We thank Kim Schuske for sharing *unc-80* cloning information. Kim Schuske, Erik Jorgensen, Steve McIntire, Terry Snutch and Philip Morgan for discussion and sharing unpublished information. We thank *C. elegans* Gene Knockout Consortium for *nca-1(gk9)* and *nca-2(gk5);* National Bioresource Project for the Nematode for *nca-1(tm1591)*; *CGC* for strains; Mike Nonet for antibodies; Bruce Bamber, Yishi Jin and Kang Shen for markers; Calvin Mok, Christine Hwang and Kyota Ayogi for experiments; Janet Richmond and John Roder for invaluable support for electrophysiology analysis. This work was supported by CIHR and NSERC grants to Mei Zhen and grants from NIDA to William Schafer. Edward Yeh held a CIHR postdoctoral fellowship.

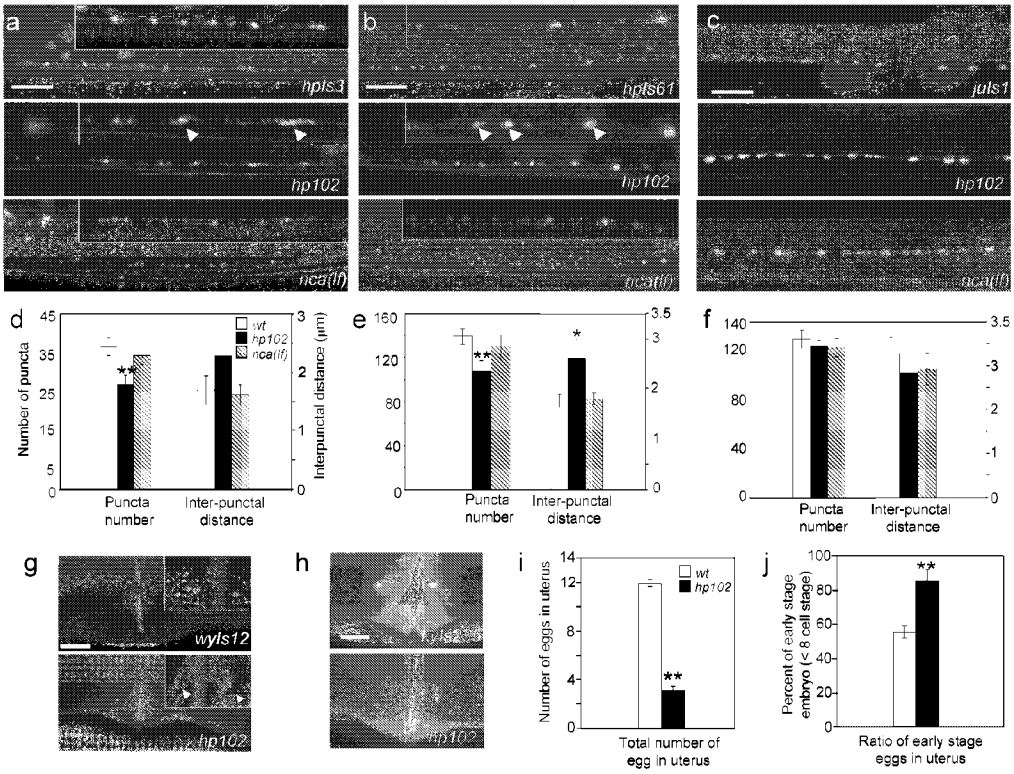

Figure 3.1:*hp102*, a gain-of-function mutation in nca-1 leads to changes in active zone morphology. a, b)Active zone morphology of dorsal GABAergic synapses in L2 larvae of wild-type, hp102 and nca(lf) animals, visualized by SYD-2::GFP (hpIs3)and UNC-10::GFP (hpIs61). Inserts are magnified views of regions marked by the dotted line. Arrowheads indicate abnormal clustering of active zone marker puncta. c) Normal vesicle morphology at GABAergic synapses visualized by SNB-1::GFP (juIs1) marker. d) Quantification of the average number (n=10 for each strain) and inter-punctal distance (n=28 for all strains) for hpIs3 (puncta at DD4-DD6 region, ~1/3 of dorsal cord region at L2 stage). e) Average number (n=15 for each strain) and inter-punctal distance (n=30, 30, 48 for wt, hp102 and nca(lf), respectively) for hpIs61 (puncta along the entire dorsal cord, L3 stage). f) Average number (n=15 for each strain) and inter-punctal distance (n=13 for all strains) for juIs1 (puncta along entire dorsal cord, n=15). g-h) Morphology of HSN synapses visualized by an active zone marker wyIs12 (g) and a vesicle marker kyIs235 (h) in wild-type (top panels) and hp102 mutants (bottom panels). i) Average number of eggs retained in uterus of hp102and wild-type animals 24hr post L4 larval stage, n=15. j) % of eggs in uterus that are in early embryonic stages (8 cells or fewer), n=15. Error bar: SEM. Statistic comparisons were performed against the wild-type dataset using the Tukey-Kramer multiple comparison test. * $p<0.01$, ** $p<0.001$, Scale bar: 5 m.

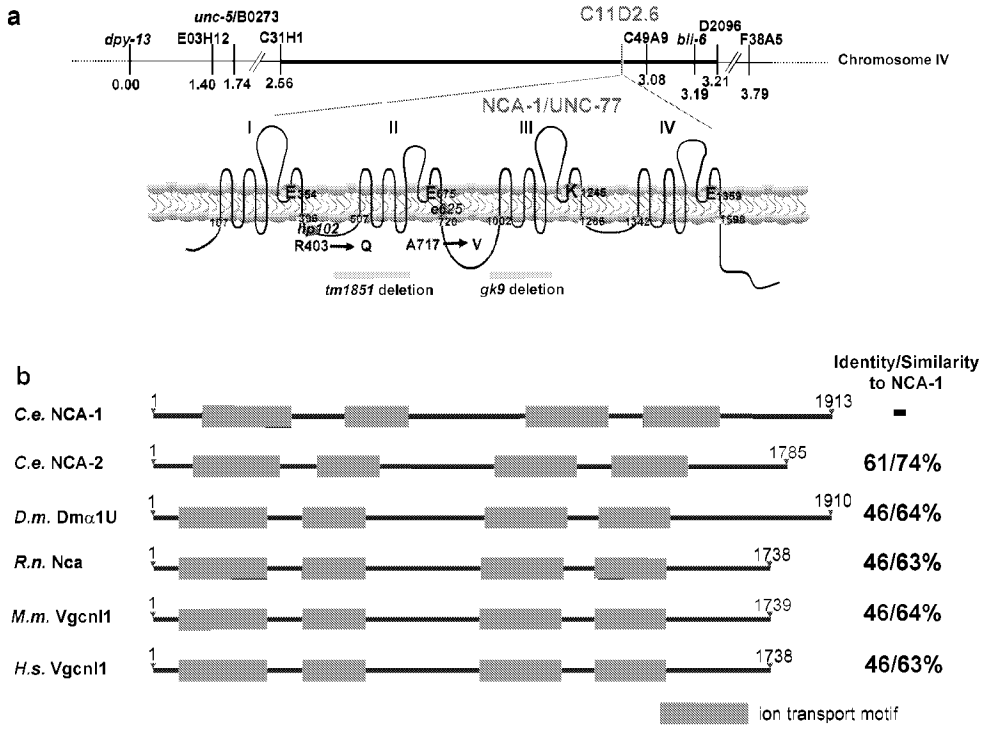

Figure 3.2: *hp102* and *e625* encode NCA-1, a cation channel α_1-like subunit. a) Genetic mapping of *nca(gf)* mutants and a schematic representation of the *nca-1* genetic locus (top) and the predicted NCA-1 protein structure (bottom). The positions of the *nca(gf)* (*hp102* and *e625*) and *nca(lf)* mutations (*gk9* and *tm1851*) are illustrated. Yellow circles denote the beginning and end of each ion transport motif. The amino acid residues that determine ion selectivity in related cation channels are highlighted with orange circles. b) Similarity between NCA family members. *C.e.*: *C. elegans*; *D.m.*: *D. melanogaster*; *R.n.*: *R. norvagicus*; *M.m.*: *M. musculus*; *H.s.*: *H. sapiens*.

Figure 3.3: Ca^{2+} transients at HSN cell bodies and synapses in *nca(lf), nca(gf)* and *unc-80* mutants. a, b) Sample traces of yellow/cyan ratio that represent the relative Ca^{2+} concentration in HSN cell bodies (cell) or their synapses (syn). X-axis: time in seconds; Y-axis: yellow/cyan ratio in %. For *nca(lf)* and *unc-80*, animals displayed traces with either silent (top) or active (bottom) Ca^{2+} transients. c-e) Histograms for the total spike frequency, spike interval, and size of calcium spikes detected in each strain. N is illustrated at the bottom of each bar. Error bar: SEM. * $p<0.05$, ** $p<0.005$. c) Average number of spikes/minute for each genotype. There is no statistically significant difference for HSN cell bodies among all strains, or between HSN cell bodies and synapses of the same strain except for *nca(lf)* and *unc-80*. d) Average time interval between two consecutive spikes within trains of calcium transients. There is no statistically significant difference between HSN cell bodies and corresponding synapses for all strains. e) Average spike size. There is no statistically significant difference between the spike size of wild-type, *nca(lf)* and *unc-80* neurons, except for the *nca-1(gf)*. f-h) Scatter plots for spike frequency, interspike time interval and spike size. Each cross represents a data point. Clear and filled triangles represent mean numbers for cell body and synapse calcium transients respectively. Red circles highlight populations of animals with silenced synapse calcium transients. Red box highlights a population of *nca(gf)* synapse spikes that were significantly larger than those seen in other genotypes. All statistic analysis was performed by Kolmogorov-Smirnov rank test.

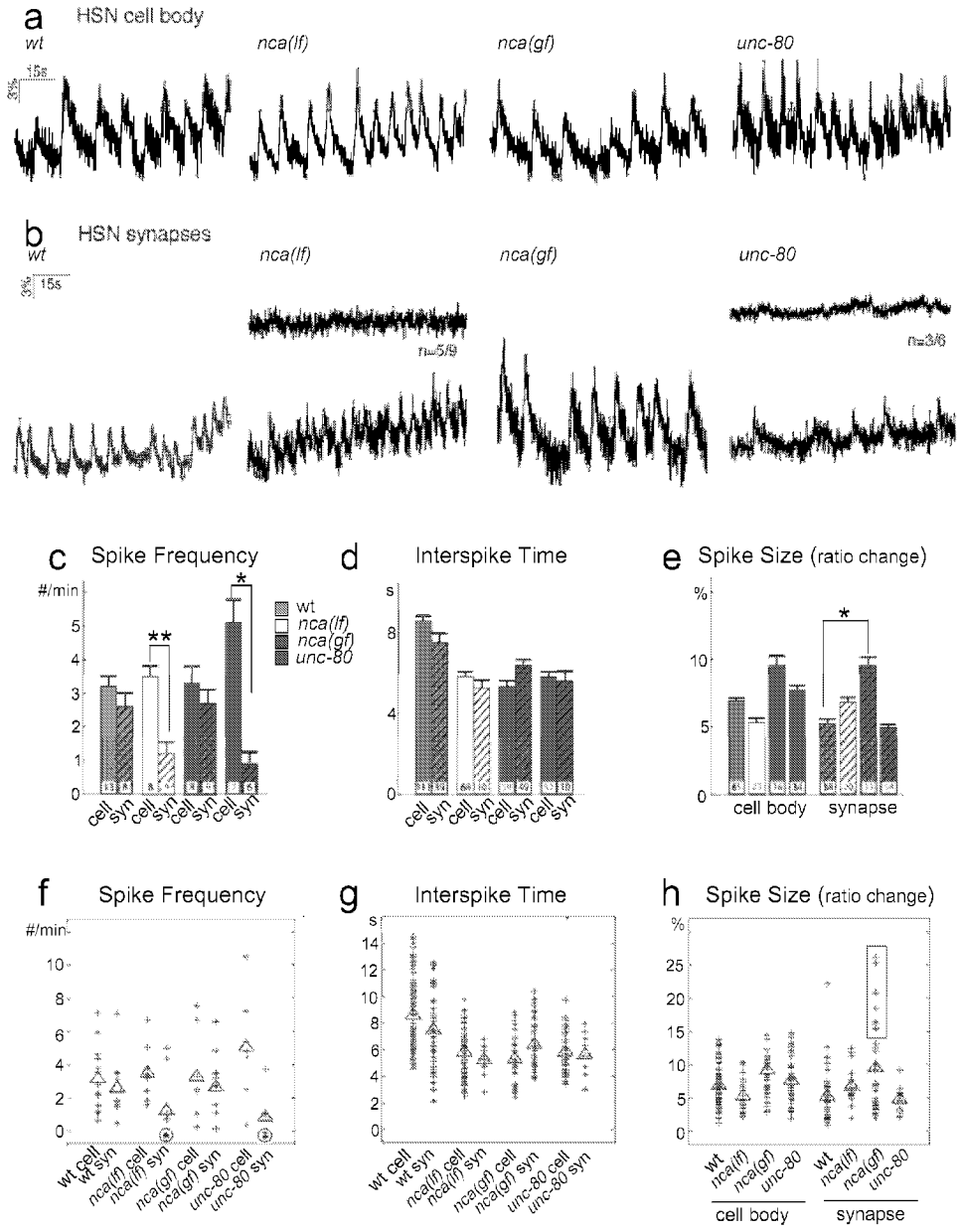
a HSN cell body
wt
nca(lf)
nca(gf)
unc-80
15s
3%
b HSN synapses
wt
nca(lf)
nca(gf)
unc-80
15s
3%
n=5/9
n=3/6
c Spike Frequency
#/min
wt
nca(lf)
nca(gf)
unc-80
cell
syn
d Interspike Time
s
e Spike Size (ratio change)
%
cell body
synapse
f Spike Frequency
#/min
wt cell
wt syn
nca(lf) cell
nca(lf) syn
nca(gf) cell
nca(gf) syn
unc-80 cell
unc-80 syn
g Interspike Time
s
h Spike Size (ratio change)
%
wt
nca(lf)
nca(gf)
unc-80
cell body
synapse

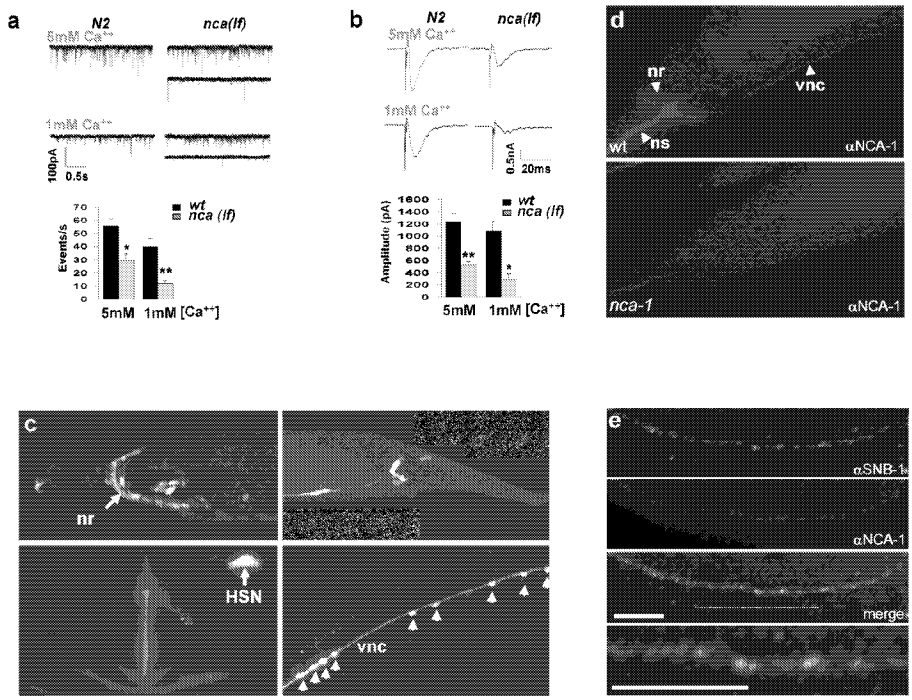

Figure 3.4: NCA-1 is required for neurotransmission and expressed in the nervous system, enriched at non-synaptic regions along axons. a) Representative traces of spontaneous activity are shown on upper part. The *nca(lf)* mutant mPSPs varied between wild-type (WT) values (upper trace) and decreased frequency and amplitude (lower trace). The overall mPSP frequency was decreased in *nca(lf)* animals as compared to wild-type at either 5mM (*nca(lf):* n=15; WT: n=13) or 1mM (*nca(lf):* n=9; WT: n=6) extracellular Ca^{2+}. b) Representative traces (upper panels) and graphical representation of the amplitude (lower panel) of the response evoked in muscle by an electrical stimulation of the ventral nerve cord for wildtype (black bars) and *nca(lf)* (grey bars) animals at 5mM (*nca(lf):* n=8; WT: n=10) or 1mM (*nca(lf):* n=6; WT: n=4) extracellular Ca^{2+}. Error bars: SEM, *$p \leq 0.01$, **$p < 0.001$. Statistic analysis was performed with student t test. c) A transcriptional GFP reporter driven by the *nca-1* promoter is active in neurons in the nerve ring (nr), neurons in the tail, HSN neuron, and ventral nerve cord (vnc) motoneurons. d) An antibody against NCA-1 shows specific staining in the nerve ring (nr) and along nerve cords in wild-type (top panel) animals that is absent in *nca-1(tm1851)* deletion mutants (bottom panel). e) Wild-type animals were co-stained with anti-NCA-1 antibody (red) and anti-SNB-1 (green). Scale bar: 5 μm.

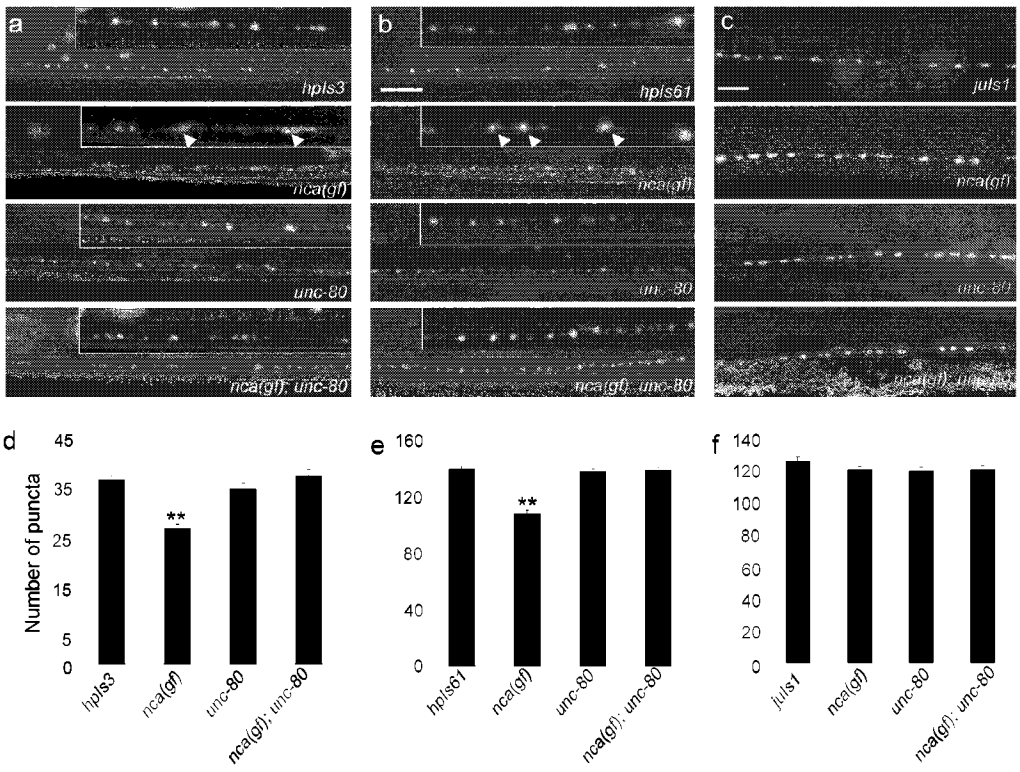

Figure 3.5: *unc-80* suppresses the active zone defects of *nca(gf)* mutants. a-c) Active zone (*hpIs3* and *hpIs61*) and vesicle (*juIs1*) morphology in wild-type, *nca-1(gf), unc-80* and *nca(gf);unc-80* animals. Inserts show magnified views of the dorsal nerve cord region marked by dotted lines. d-f) Quantification of active zone and vesicle punctum number in wild-type, *nca-1(gf), unc-80* and *nca(gf);unc-80* animals as in Figure1: d) *hpIs3*, n=10, e) *hpIs61*, n=15, f) *juIs1* n=15. Error bar: SEM. Scale bar: 5 μm. **p<0.001.

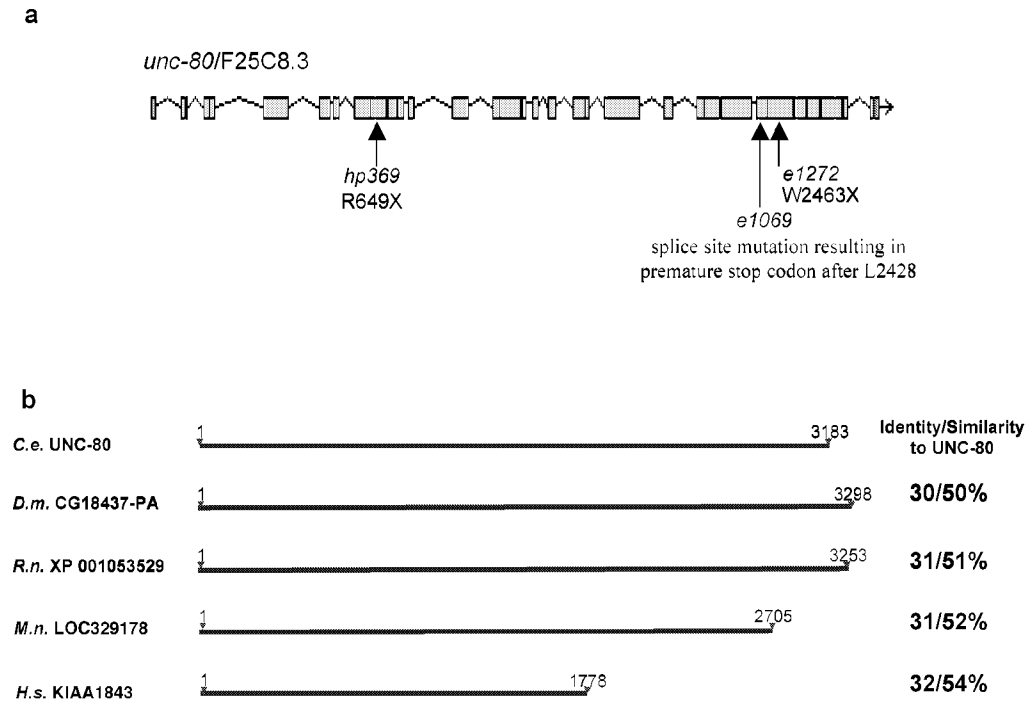

Figure 3.6: UNC-80 is a highly conserved novel protein. a) A schematic representation of the gene structure of *unc-80 (F25C8.3)* adapted from Wormbase. The exons are shown as pink boxes. The genetic lesions of *unc-80* alleles (*e1069, e1272* and *hp369*) are shown. b) Protein structure and similarity of UNC-80 family members. *C.e.*: *C. elegans*; *D.m.: D. melanogaster*; *R.n.: R. norvagicus*; *M.m.: M. musculus*; *H.s.*: *H. sapiens*.

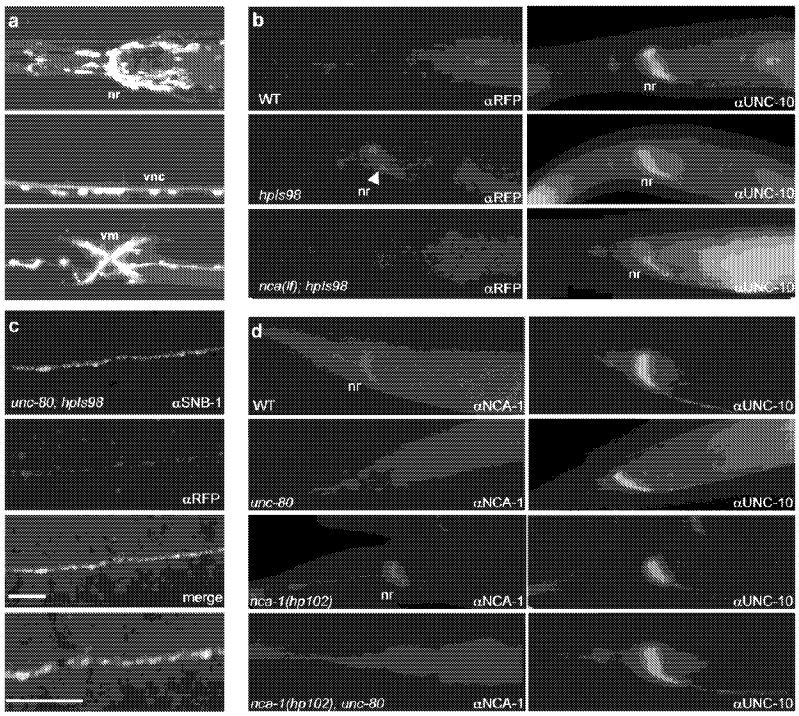

Figure 3.7: UNC-80 and NCA-1 share similar expression pattern, and depend on each other for localization. a) A transcriptional GFP reporter driven by the *unc-80* promoter activates expression in neurons in the head and nerve ring (nr), motoneurons in the ventral nerve cord (vnc), neurons in tail, and vulva muscles (vm). b) Staining with anti-RFP antibodies in wild-type (negative control), *hpIs98* (UNC-80::RFP) and *nca(lf);hpIs98* animals (left panels). Specific nerve ring staining (arrow) of UNC-80::RFP disappeared in *nca(lf)* animals. UNC-10 staining is present in the same animals (right panels). c) *unc-80;hpIs98* animals co-stained with anti-RFP antibody (red) and anti-SNB-1 (green) showed poor co-localization. d) Wild-type (WT), *unc-80(e1272), nca-1(hp102)* and *hp102; unc-80* animals co-stained with anti-NCA-1 (red) and anti-UNC-10 antibodies (green, as staining control). NCA-1 staining is present in *hp102* but disappeared in *unc-80* and *hp102;unc-80* animals. Scale bar: 5 μm.

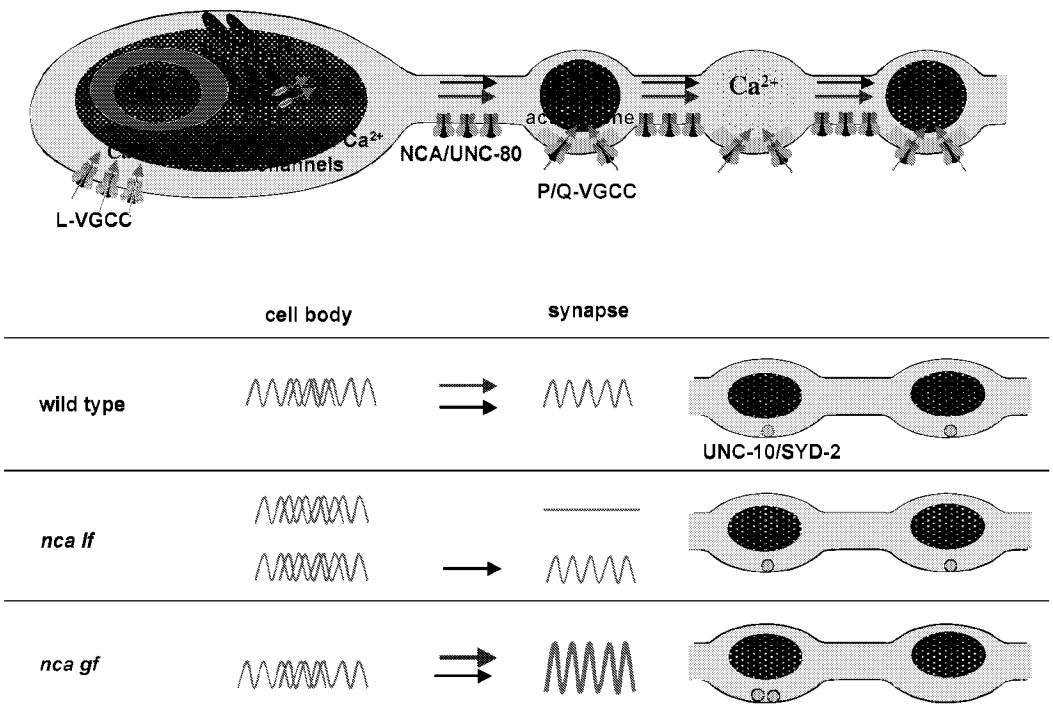

Figure 3.8: Model of NCA-1/UNC-80 function in neurons. Top - A schematic representation of a *C. elegans* neuron with *en passant* synapses. Ca^{2+} transients in the cell body are likely contributed by influx from L-type VGCCs and release from intracellular calcium pools. At the synapse, depolarization signals (red waves) initiate calcium influx through P/Q-type VGCCs at the active zone. NCA/UNC-80 complexes regulate membrane excitability along the axon to allow the propagation of some depolarization signals. Bottom - In *nca(lf)* mutants some depolarization signals fail to propagate along the axon while others can still reach synapses. In *nca(gf)* mutants the signals are amplified, resulting in increased synaptic activity, which indirectly regulates active zone component distribution.

This Chapter is a currently submitted draft which format is adapted to this thesis. Yeh E*, Ng S*, Zhang M*, Bouhours M, Wang Y, Hung W, Melnik-Martinez K, Li M, Schafer WR and Zhen M are among the author list of "A voltage-Gated Cation Channel-like Protein NCA-1 and a Novel Protein UNC-80 Regulate Synaptic Activity and Development in C. elegans". I am one of the three co-first authors and did all the neural imaging experiments that showed the NCA channel functions at the excitation spreading from the cell body to synapses in the HSN cell to affect egg-laying behavior.

CHAPTER IV: A THEORETICAL MODEL ON THE TEMPORAL PATTERN OF *CAENORHABDITIS ELEGANS* EGG-LAYING BEHAVIOR

ABSTRACT

Egg-laying in the nematode *C. elegans* displays a clustered temporal pattern , providing an opportunity to study the neural mechanism of pattern generation in a simple model organism. The circuitry mechanism that excites the motor program to produce individual egg-laying events has been characterized and reported in the Chapter II. Here we propose a theoretical model on the temporal pattern in egg-laying based on statistical analyses and genetic experiments. We suggest that the HSN cell is the command neuron of egg-laying; the VC cell works as the "single egg counter" that after being activated by individual egg-laying events inhibits the HSN activity for a short period of about 20 seconds; and the uv1 is the "cluster egg counter", activated by a cluster of egg-laying events happening close to each other and then inhibiting the HSN activity for longer periods of about 20 minutes. Experiments for testing this model are also suggested.

INTRODUCTION

Instead of just being randomly aroused, very often a behavior is under regulation that gives a certain temporal pattern. Even the simple nematode displays different temporal patterns in several behaviors; for example, a clustered pattern is observed for egg-laying, and a highly periodic pattern is seen for defecation. Understanding the neural mechanisms behind pattern generation in the nervous system has been challenging due to

its complexity. Here we took the opportunity of studying in the pattern generating mechanisms for egg-laying in the relatively simple but extensively characterized nervous system of *C. elegans*.

Egg-laying behavior in *C. elegans* displays a clustered temporal pattern: several eggs are laid quickly in short periods, which are called active states, and interspaced by long silent periods of time called inactive states. Within an active state, the individual egg-laying events are called egg-laying states, although it is not clear whether or not it is a maintainable situation. Time intervals between two consecutive egg-laying events within active states are short, on average about 20 seconds, while those between active states are longer, about 20 mins in wild type animals. Mathematically, they roughly follow two random point Poisson processes with different time constants ($\lambda 1$ and $p*\lambda 2$), and the whole egg-laying behavior is switching between inactive state and the active state with the possibility of p (Zhou et al., 1998);

The neural mechanism producing individual egg-laying events has been characterized as in the Chapter II. Individual spikes in the HSN motorneurons drive an immediate egg-laying event by exciting the vulval muscles. The VC motorneurons provide a redundancy in exciting the vulval muscles after being activated by the HSNs and also exert a negative feedback effect back onto the HSN activity, though the physiological significance of this feedback loop isn't clear yet.

Besides the core egg-laying circuit (the HSNs, VCs and vulval muscles) which has a direct excitatory influence on egg-laying, additional cells may have modulatory or inhibitory effects. The PLM posterior mechanoreceptor neuron has been shown to inhibit egg-laying very transiently, but PLM is not an essential element for egg-laying

behavioral regulation. The uv1 epithelial cells have also been found to have a negative effect on the overall egg-laying rate, perhaps upon activation by its TRPV potential touch receptors (Jose et al., 2007). They are hypothesized to sense egg accumulation status within the uterus via touch sensing, but their interactions with the core egg-laying circuit are not clear.

Behavioral regulation involves multiple neurons interacting with each other in a non-linear and dynamic way upon changing conditions. Theoretical efforts are useful in summarizing the current data and more importantly for presenting new hypotheses for future experimentation. Here we performed statistical analyses on the egg-laying circuit activity in different genetic backgrounds in order to build up a theoretical model for the clustered temporal pattern of *C. elegans* egg-laying behavior.

RESULTS

The VCs are responsible for short inhibitions within active states

The motorneuron HSN appears to function as the command neuron for egg-laying behavior; therefore any modulation on its activity will have similar effects to the overall behavior. The VCs have been shown in Chapter II to down-regulate the HSN activity (Figure 4.1A); here we further analyzed their effect on the temporal pattern in the HSN spikes. In our imaging experiments, due to the time constraint of our facility, we can record a maximum of 10 minutes (ln10=2.30) of HSN activity; thus the spike intervals longer than that, corresponding the long intervals in the log probability, are missed. The HSN activity in wt displays a spread in its interval distribution comparable to that in wt behavior, suggesting that the HSN activity in wt animals may also roughly follow random

Poisson process. The HSN activity in *lin-39* worms displays a higher frequency with a narrower distribution of interval times that has been confirmed statistically to be highly periodic: all the intervals follow a normal distribution for each single worm ($p<0.05$), indicating a uniformly maximum activity (Figure 4.1B). This result suggests that the VC cell may negatively regulate HSN activity within the active phase of egg-laying. Consistent with this, the HSN spike intervals larger than 30 seconds are very rare in *lin-39* worms as shown in the logtail probability graph (Figure 4.1C).

Individual egg-laying events feed back on the HSN and VC activities

Previously, egg-laying events were shown to be coupled with Ca^{2+} spikes in both the HSNs and VCs. Closer examination found that they are specifically coupled with peak-ends of the Ca^{2+} spikes if the spike frequency is below an subjectively chosen threshold 1/min, which is true for both HSN and VC cells (Figure 4.2A; 4.3A, 4.3B). This suggests that egg-laying events, after induced by a depolarization in both HSN and VC cells, may actively terminate the depolarization in those cells. It isn't clear which cell, either HSN or VC or both redundantly, might directly sense successful egg-laying events and if only one cell dose so, how it might shut off its own and the other cell'sactivity. One possibility is that the VCs actively shut down their own activity as well as that of the HSNs after an egg-laying event and continue to inhibit it for a short period. This model is consistent with the data that the correlation between egg-laying and VC spike ends are stronger than that between egg-laying and HSN spike ends (the slope in regards to VC-egglaying is 0.926, more close to the theoretical "1" than that of 0.85 for the HSN. And p is smaller for the VCs (<0.001) than that for the HSNs (<0.05)). All of the above analyses and speculations are based on overall cellular activities in Ca^{2+}

dynamics revealed by neural imaging, and do not suggest a possible molecular mechanism by which either the HSN and/or VC cells might sense egg-laying events.

The uv1 cells may inhibit HSN activity for longer periods corresponding to the inactive egg-laying state

In *lin-39(n709ts)* mutant animals, HSN activity still showed long periods of silence, which may correspond to the inactive state in egg-laying. The transition of HSN activity from oscillatory activity to silence and from silence to oscillatory activity are both caught in single recordings (Figure 4.4B). Therefore the VCs appear to be only responsible for short inhibitions within the active state, and some other mechanism may be responsible for regulating the inactive state in egg-laying. The uv1 cells have been found to strongly inhibit egg-laying, an effect which may involve TRPV putative touch channels. The fact that they are touch sensitive also inspired us to wonder that they may also respond to osmolarity and mediate its effect on egg-laying. To examine this possibility, we tested a uv1-defective mutant, in which the uv1 cells are always silent due to a dominant negative mutation in one TRPV channel subunit, *ocr-2(vs29).* The *ocr-2* animals are strongly egg-laying constitutive due to the defective uv1 cells, and our experiment showed that egg-laying in these mutant animals is not inhibited by high osmolairy buffer M9 (Figure 4.4A). This result suggests that the uv1 cells may mediate the osmolarity's effect on egg-laying and the high and low osmolarity conditions correspond to uv1 active and silent situations respectively.

As the HSN also responds to osmolarity changes, it is highly possible that the HSN may be downstream of the uv1 cells. Since the uv1s use neuropeptides and are close enough to the HSN cells to signal to them in a paracrine fashion, it is quite possible

that HSN is the direct target of the uv1 neuromodulators. Consistent with this possibility, while HSN is almost completely silenced in high osmolarity conditions (Figure 4.4B), in low osmolarity conditions, we sometimes see worms that are silent at the beginning of the trace but then become activeuntil the end of the recording (Figure 4.4B). The fact that low osmolarity can cause a switch between uniformly oscillating and silent HSN activity suggests that the low and high osmolarity conditions may correspond to the egg-laying and inactive states respectively. The uv1 cells might be responsible for inducing inactive states in HSN. Consistent with this, egg-laying behavior also showed almost silence in high osmolarity conditions (1~2 eggs/min), while in low osmolarity conditions almost all the eggs contained in the uterus were expelled within 15 mins.

The uv1 cells are hypothesized to activate upon a cluster of egg-laying events

The uv1 cells are thought to be activated by its touch channels, but the physiological stimulus that triggers its touch sensation aren't clear yet. The uv1 cells are located among a series of epithelial cells, uv1-uv3, connecting between the uterus and the vulva, and the uv1s are the most close to the vulva. The uv1 cells send out short processes forming a tight enclosure around the vulva, which may potentially constitute a touch-sensitive specialization (Figure 4.4C). The uv1 cells could be quite sensitive to the mechanical distortion around the vulva that is induced by eggs passing through the vulva passage in successful egg-laying events. Since the uv1 cells use neuropeptides, which diffuse in the extra-cellular spaces with slow kinetics, we hypothesize that the uv1's may be activated by one or more egg-laying events, which could then lead to the release of inhibitory neuropeptides that induce the inactive state.

Overall model for the egg-laying circuit

Together, our model on the clustered temporal pattern in egg-laying is as follows: The HSN cells is the command neuron for egg-laying with its individual Ca^{2+} spikes corresponding to one egg-laying event. The VC cells work as "single egg counters" that are activated by individual egg-laying events and then inhibit the HSN activity for short periods of about 20 seconds on average. Finally, the uv1 cells are the "cluster egg counters", activated by a cluster of egg-laying events and inhibiting HSN activity for longer periods of about 20 minutes on average. In our model, the VC and uv1 cell form two negative feedback loops connecting from egg-laying behavior back onto the HSN activity; however, they are different in the physiological activations and when activated, in different time constants in inhibiting HSN activity. Altogether these two feedback loops formulate a clustered temporal pattern displayed in egg-laying.

DISCUSSIONS

The model we presented here is so far the simplest to explain all current data, however its validation waits further testing. We suggest using vulva developmental mutants, which are incapable in accomplishing egg-laying, to confirm the existence of negative feedback loops. Also, the activity of the uv1 cells can be imaged using cameleon to see whether or not they are activated by egg-laying events. If the VCs directly sense egg-laying events, they might be expected to contain touch sensitive channels which could be identified.

Previously, the clustered temporal pattern in egg-laying is simulated mathematically as two Poisson processes with different time constants ($\lambda 1$, $p*\lambda 1$) and a

switching probability p. The model we developed from biological evidence fits to that mathematical description surprisingly well and even helps assign specific biological pathways for each parameter. The Poisson-like nature of both long and short interval distributions can be explained as the HSN cells randomly switching to the egg-laying state after being inhibited by either the VCs or the uv1s; the intra- and inter-cluster time constants correspond to that two switching possibilities respectively. The p probability in the mathematical simulation corresponds to how many egg-laying events of a cluster is required to activate the uv1 pathway, which is determined by the distance between the HSN and uv1 cells and also the diffusion constant in the extracellular space between them.

The temporal pattern in egg-laying may underlie other behaviors or in other organisms. For example, sleeping is an alternation between two states, awake and asleep. This temporal pattern corresponds to partial the temporal pattern in our studied *C. elegans* egg-laying, probably the alternation between overall active and inactive states. The "mood" is also a phenomenon of jumping from states to states. For *C. elegans* egg-laying, the two-cell circuits, uv1-HSN and VC-HSN, manage the state alternating. It is interesting to see whether or not same structured circuits are employed in those similarly patterned behaviors.

The HSNs can be seen as an information integration center, processing signals from uv1, VC cells on top of its own autonomous activity. It functions as a "Nor" gate here, giving the output of "1" only if both VC and uv1 are inactive. Computers are built up from four basic computational units, so called "and", "or", "nor" and "nand" gates. Are there similar computational units also behind the biological intellects? The HSNs is

a nice system for more detailed study of this "Nor" calculation, which may have intriguing implications in general biology computations.

METHODS AND MATERIALS

General Methods

All nematodes were grown at 20.5±0.5°C on standard Nematode Growth Medium (NGM) seeded with *E. coli* strain OP50 as the food source. Nematodes were assayed 24 hours after late L4 stage at 20.5±0.5°C.

Egg-laying Behavior Assays

M9 egg-laying assays were performed in 96-well plates. 100 µl of melted 2% agarose in M9 were placed in each well and allowed to dry for 1~1.5 hours before starting the behavioral assay. Individual worms were placed on the solid agarose pad in each well and after about 1 min were covered with 50 µl of M9. The number of laid eggs were counted after 1.5 hours.

Ca2+ Imaging Experiments

The protocol is the same as described in Chapter Two. Combined fluorescent and visible microscopy was used to view both the Ca^{2+} signal and egg-laying events simultaneously. The microscope equipment was as described in Suzuki's paper (Suzuki et al., 2003), briefly, a Zeiss Axioskop 2 upright microscope equipped with a Hamamatsu Orca ER CCD camera, a Hamamatsu W-View emission image splitter and a Uniblitz Shutter (Vincent Associates). A minimum of fluorescent light, 20-60% of the original light power with the neutral density filter (ND) of 2.0, was used. Weak visible light, barely revealing egg-laying events, was used to minimize interference with the cameleon

fluorescent signal. Fluorescent images were acquired and saved using MetaVue 4.6 (Universal Imaging) at a frequency of either 33hz or 10 Hz for muscle and neuron imaging respectively (binning 4X4), using a 63X Zeiss Achroplan water immersion objective.

Worms were immobilized with Nexaband S/C cyanoacrylate veterinary glue on a small agarose pad with the buffer of choice freshly made on a microscopy slide. The worms were then quickly covered with the buffer of choice and immediately moved under the microscope for recording. For HSN and vulval muscle imaging, the agarose pad was made in the same buffer as the bath. For VC imaging, a 2% agarose pad in M9 was used, regardless of the bath buffer, due to the fast adaptation of VCs to low osmolarity conditions. Agarose pads were made immediately before slide preparation in order to minimize the loss of focus in long recordings (10 mins), which usually is caused by swelling of the agarose pad. Worms were allowed to equilibrate for two-four mins before the start of recording.

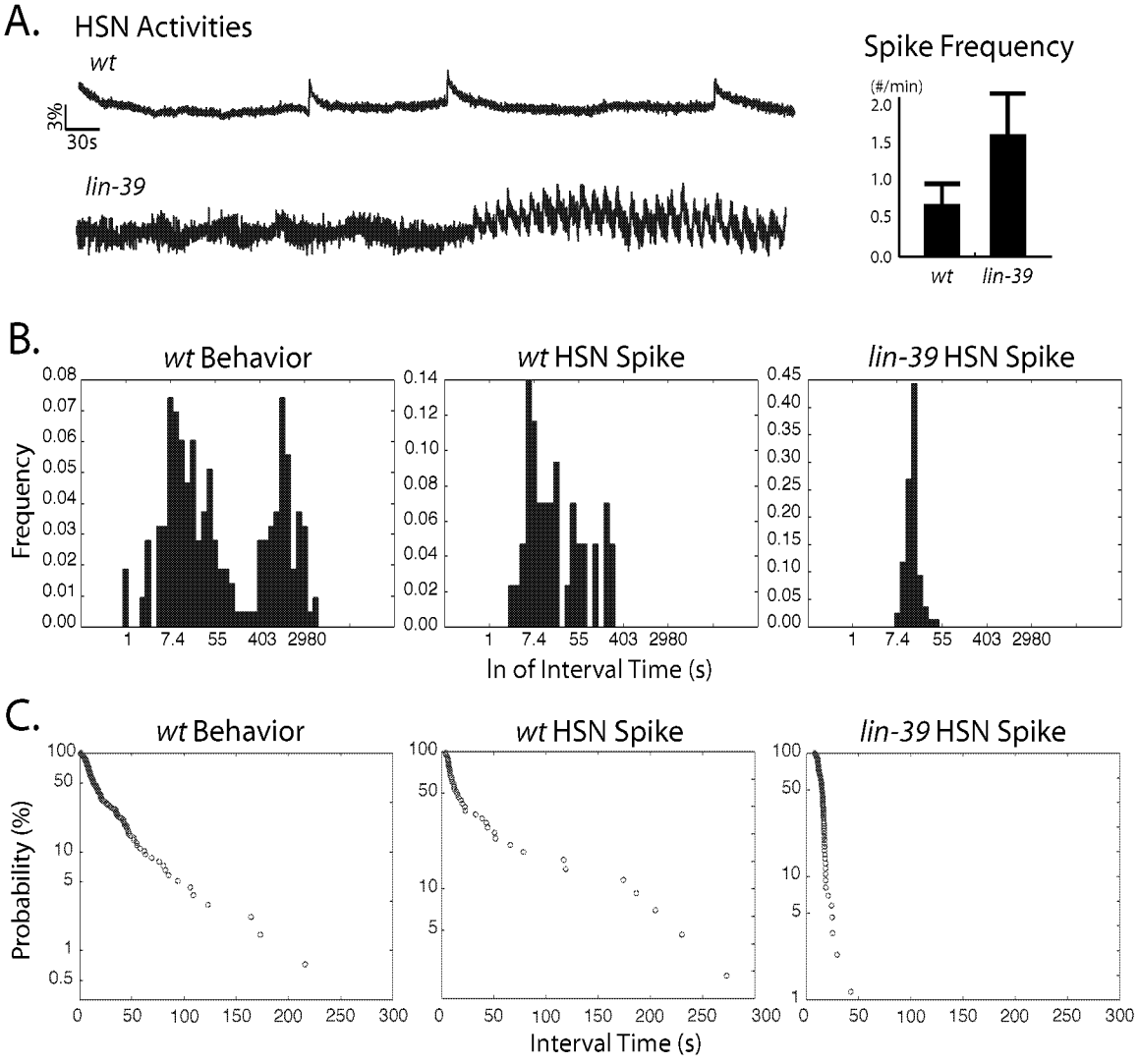

Figure 4.1: VC affects HSN activity. A) The lack of VCs causes increased spike frequencies in HSN activitiy. Sample traces of HSN in wild type and *lin-39* animals are shown. The overall spike frequencies are summarized in the bar graph. B) The ditributions of ln interval times for the egg-laying behavior in *wt*, HSN spikes in *wt* and *lin-39* animals. C) The log tail probability graph for egg-laying behavior in *wt*, HSN spikes in *wt* and *lin-39* worms.

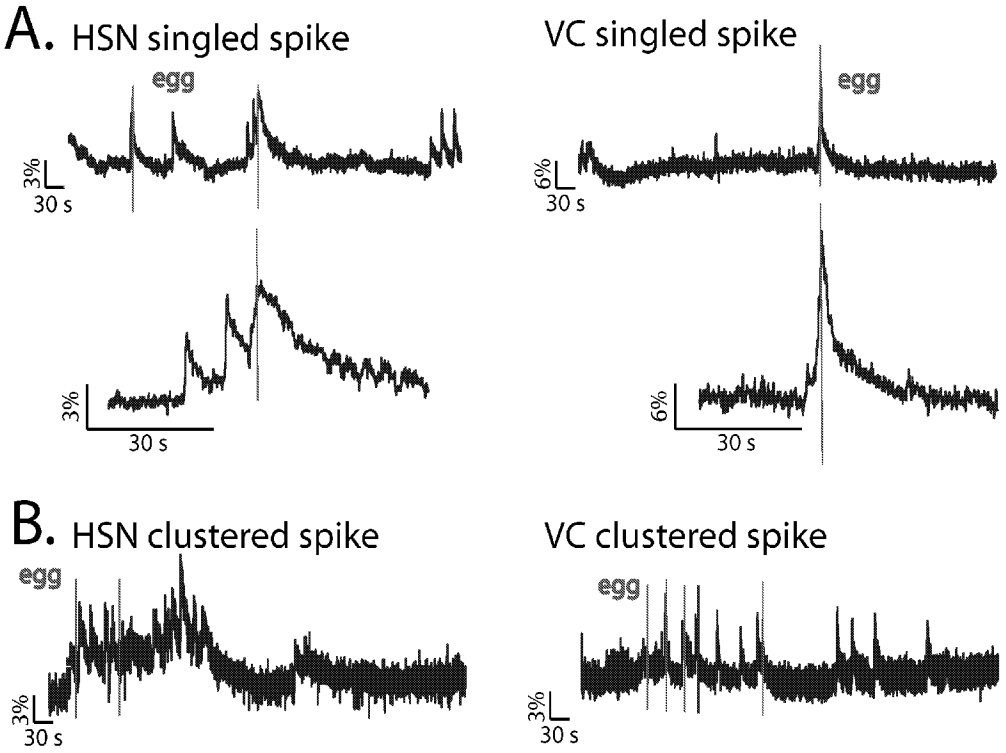

Figure 4.2: Sample traces for the coupling between egg-laying events and Ca^{2+} spikes in both HSN and VC cells. A) The sample traces when the overall spike frequency is below 1/min. B) The sample traces when the overall spike frequency is higher than 1/min.

Figure 4.3: The correlation between egg-laying and spike ends in HSN and VC cells. The meanings of the numbers used in calculations are as indicated in D). A,B) The correlation between egg-laying and spike ends, between spike ends and rising slope, between spike ends and the overall ratio change and that between the rising slope and the overall ratio change for HSN and VC cells when the spike frequency is below 1/min are calculated and shown. C) The correlation between egg-laying and spike ends for HSN and VC cells when the spike frequency goes higher than 1/min are calculated and shown.

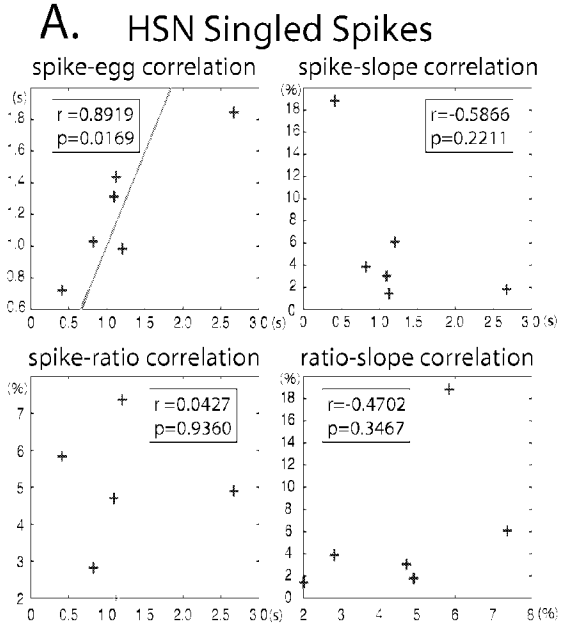

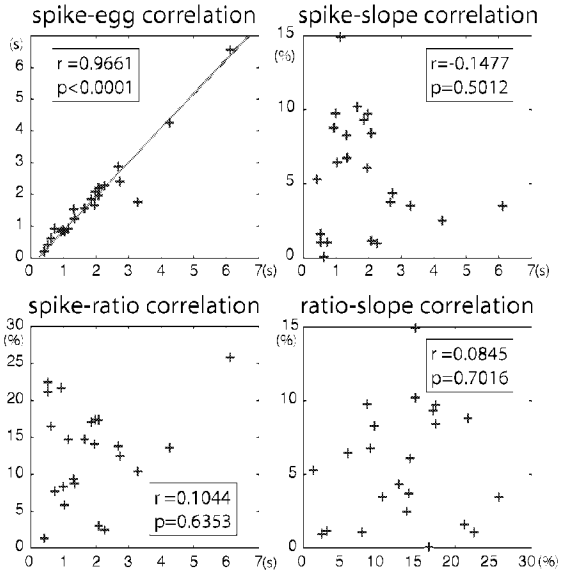

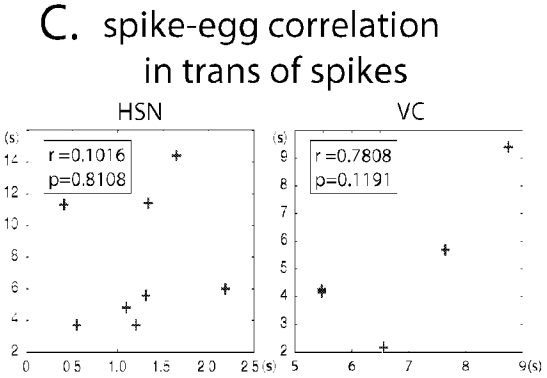

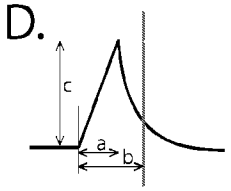

a,'spike' duration.
b,'egg'-laying timing.
c, spike 'ratio' change.
d=c/a, spike 'slope'.

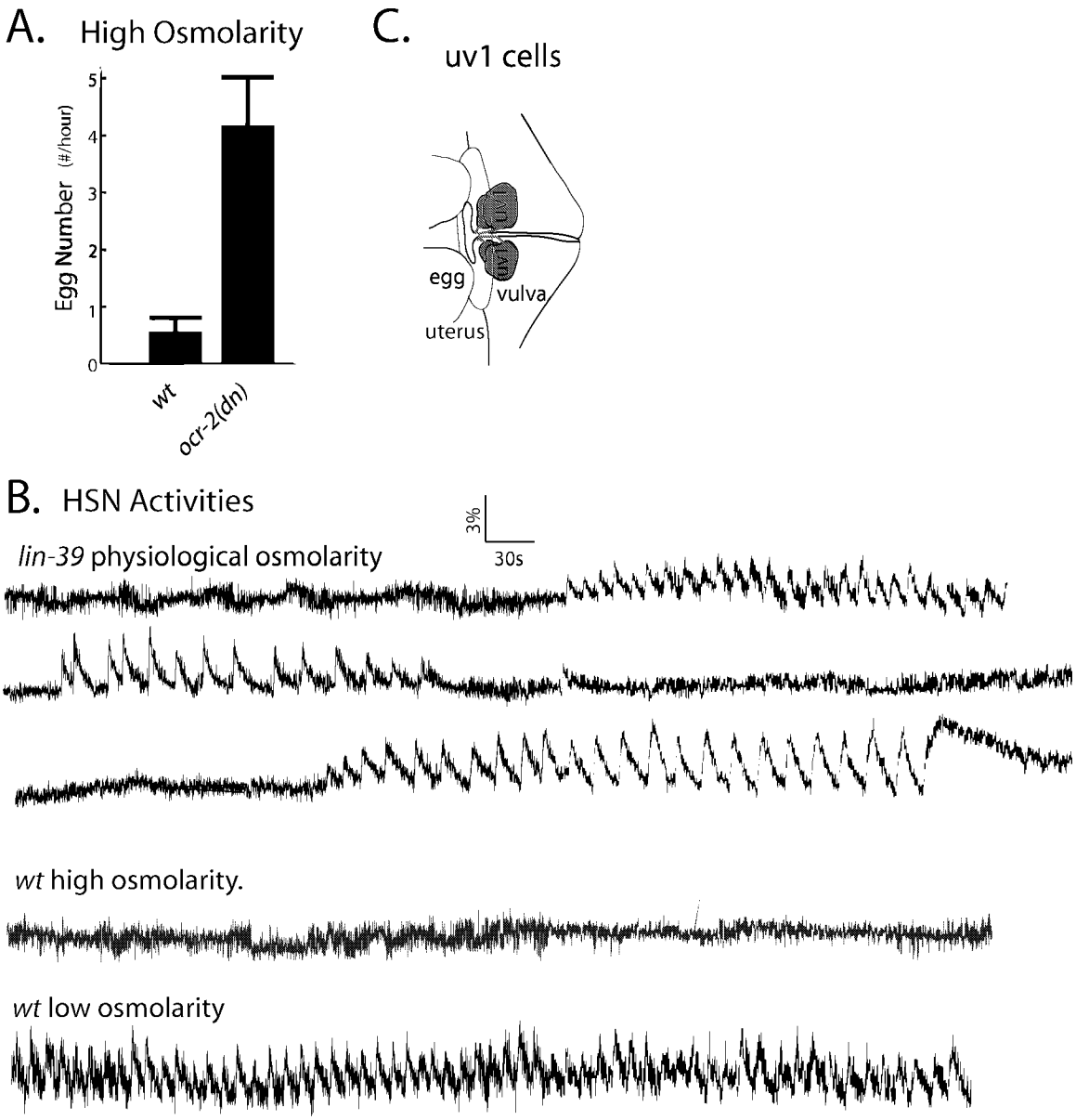

Figure 4.4: uv1 cell may regulate the overall active and inactive states and its morphology. A) The *ocr-2(dn)* mutant animals are not inhibited by high osmolarity M9 buffer. B) The HSN activity revealed by cameleon signal shows uniformly silence and oscillatory activities in high and low osmolarity conditions respectively. Scale bars are as indicated. C) The morphology of uv1 cells.

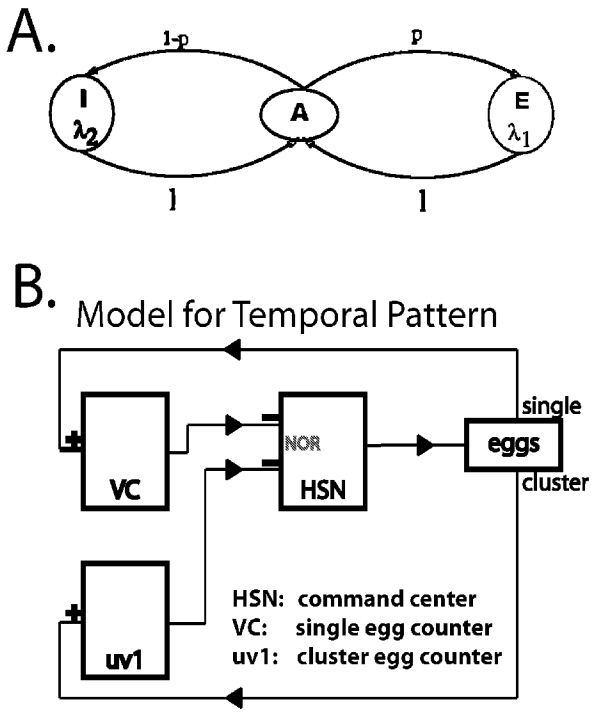

Figure 4.5: The overall model for the clustered temporal pattern behind *C. elegans* egg-laying. A) Three state model for egg-laying. I = inactive state. A = active state. E = egg-laying state. The A → E transition occurs with probability p, and its time constant is λ1. The A → I transition occurs with probability q = 1-p, and its time constant is λ2" (Zhou et al., 1998). B) The overall model on the clustered temporal pattern. "Eggs" in square boxes represent the behavior. "Single" stands for single successful egg-laying events. "Cluster" stands for clustered egg-laying behavior. "+" is for a positive effect and "-" is for a negative

This part of text is going to be submitted to a peer-review journal. The author list includes Mi Zhang, Rainer Breitling, Rex Kerr and William R. Schafer. I am the primary researcher and author for this chapter.

REFERENCES

Bany, I.A., Dong, M.Q., and Koelle, M.R. (2003). Genetic and cellular basis for acetylcholine inhibition of Caenorhabditis elegans egg-laying behavior. J Neurosci *23*, 8060-8069.

Bargmann, C.I., and Avery, L. (1995). Laser killing of cells in *Caenorhabditis elegans*. *Meth. Cell Biol. 48*, 225-250.

Bergman, H., and Deuschl, G. (2002). Pathophysiology of Parkinson's disease: from clinical neurology to basic neuroscience and back. Mov Disord *17 Suppl 3*, S28-40.

Brenner, S. (1974). The genetics of Caenorhabditis elegans. Genetics *77*, 71-94.

Brockie, P.J., Mellem, J.E., Hills, T., Madsen, D.M., and Maricq, A.V. (2001). The *C. elegans* glutamate receptor subunit NMR-1 Is required for slow NMDA-Activated currents that regulate reversal frequency during locomotion. Neuron *31*, 617-630.

Cangiano, L., and Grillner, S. (2005). Mechanisms of rhythm generation in a spinal locomotor network deprived of crossed connections: the lamprey hemicord. J Neurosci *25*, 923-935.

Catterall, W.A. (1999). Interactions of presynaptic Ca2+ channels and snare proteins in neurotransmitter release. Ann N Y Acad Sci *868*, 144-159.

Catterall, W.A. (2000). Structure and regulation of voltage-gated Ca2+ channels. Annu Rev Cell Dev Biol *16*, 521-555.

Catterall, W.A., Perez-Reyes, E., Snutch, T.P., and Striessnig, J. (2005). International Union of Pharmacology. XLVIII. Nomenclature and structure-function relationships of voltage-gated calcium channels. Pharmacol Rev *57*, 411-425.

Chen, F., Hersh, B.M., Conradt, B., Zhou, Z., Riemer, D., Gruenbaum, Y., and Horvitz, H.R. (2000). Translocation of C. elegans CED-4 to nuclear membranes during programmed cell death. Science *287*, 1485-1489.

Chung, S.H., Clark, D.A., Gabel, C.V., Mazur, E., and Samuel, A.D. (2006). The role of the AFD neuron in C. elegans thermotaxis analyzed using femtosecond laser ablation. BMC neuroscience *7*, 30.

Colavita, A., Krishna, S., Zheng, H., Padgett, R.W., and Culotti, J.G. (1998). Pioneer axon guidance by UNC-129, a C. elegans TGF-beta. Science *281*, 706-709.

Conradt, B., and Horvitz, H.R. (1998). The C. elegans protein EGL-1 is required for programmed cell death and interacts with the Bcl-2-like protein CED-9. Cell *93*, 519-529.

Couteaux, R., and Pecot-Dechavassine, M. (1970). [Synaptic vesicles and pouches at the level of "active zones" of the neuromuscular junction]. C R Acad Sci Hebd Seances Acad Sci D *271*, 2346-2349.

Coyle, I.P., Koh, Y.H., Lee, W.C., Slind, J., Fergestad, T., Littleton, J.T., and Ganetzky, B. (2004). Nervous wreck, an SH3 adaptor protein that interacts with Wsp, regulates synaptic growth in Drosophila. Neuron *41*, 521-534.

Desai, C., Garriga, G., McIntire, S., and Horvitz, H.R. (1988a). A genetic pathway for the development of the *Caenorhabditis elegans* HSN motor neurons. Nature *336*, 638-646.

Desai, C., Garriga, G., McIntire, S.L., and Horvitz, H.R. (1988b). A genetic pathway for the development of the Caenorhabditis elegans HSN motor neurons. Nature *336*, 638-646.

Desai, C., and Horvitz, H.R. (1989). Caenorhabditis elegans mutants defective in the functioning of the motor neurons responsible for egg laying. Genetics *121*, 703-721.

Duerr, J.S., Frisby, D.L., Gaskin, J., Duke, A., Asermely, K., Huddleston, D., Eiden, L.E., and Rand, J.B. (1999). The *cat-1* gene of *Caenorhabditis elegans* encodes a vesicular monoamine transporter required for specific monoamine-dependent behaviors. J. Neurosci. *19*, 72-84.

Franks, C.J., Pemberton, D., Vinogradova, I., Cook, A., Walker, R.J., and Holden-Dye, L. (2002). Ionic basis of the resting membrane potential and action potential in the pharyngeal muscle of Caenorhabditis elegans. J Neurophysiol *87*, 954-961.

Frokjaer-Jensen, C., Kindt, K.S., Kerr, R.A., Suzuki, H., Melnik-Martinez, K., Gerstbreih, B., Driscol, M., and Schafer, W.R. (2006). Effects of voltage-gated calcium channel subunit genes on calcium influx in cultured C. elegans mechanosensory neurons. J Neurobiol *66*, 1125-1139.

Garner, C.C., Kindler, S., and Gundelfinger, E.D. (2000). Molecular determinants of presynaptic active zones. Curr Opin Neurobiol *10*, 321-327.

Goodman, M.B., Hall, D.H., Avery, L., and Lockery, S.R. (1998). Active currents regulate sensitivity and dynamic range in C. elegans neurons. Neuron *20*, 763-772.

Grillner, S. (2003). The motor infrastructure: from ion channels to neuronal networks. Nature reviews *4*, 573-586.

Hellgren, J., Grillner, S., and Lansner, A. (1992). Computer simulation of the segmental neural network generating locomotion in lamprey by using populations of network interneurons. Biological cybernetics *68*, 1-13.

Hill, A.A., Masino, M.A., and Calabrese, R.L. (2003). Intersegmental coordination of rhythmic motor patterns. Journal of neurophysiology *90*, 531-538.

Hille, B. (2001). Ion Channels of Excitable Membranes (Sunderland, MA: Sinauer Associates Inc.).

Horvitz, H.R., Chalfie, M., Trent, C., and Evans, P.D. (1982a). Serotonin and octopamine in the nematode *Caenorhabditis elegans*. Science *216*, 1012-1014.

Horvitz, H.R., Chalfie, M., Trent, C., Sulston, J.E., and Evans, P.D. (1982b). Serotonin and octopamine in the nematode Caenorhabditis elegans. Science *216*, 1012-1014.

Humphrey, J.A., Hamming, K.S., Thacker, C.M., Scott, R.L., Sedensky, M.M., Snutch, T.P., Morgan, P.G., and Nash, H.A. (2007). A putative cation channel and its novel regulator: cross-species conservation of effects on general anesthesia. Curr Biol *17*, 624-629.

Hung, W., Hwang, C., Po, M.D., and Zhen, M. (2007). Neuronal polarity is regulated by a direct interaction between a scaffolding protein, Neurabin, and a presynaptic SAD-1 kinase in Caenorhabditis elegans. Development *134*, 237-249.

Jin, Y., Jorgensen, E., Hartwieg, E., and Horvitz, H.R. (1999). The Caenorhabditis elegans gene unc-25 encodes glutamic acid decarboxylase and is required for synaptic transmission but not synaptic development. J Neurosci *19*, 539-548.

Jose, A.M., Bany, I.A., Chase, D.L., and Koelle, M.R. (2007). A specific subset of transient receptor potential vanilloid-type channel subunits in Caenorhabditis elegans endocrine cells function as mixed heteromers to promote neurotransmitter release. Genetics *175*, 93-105.

Jospin, M., Jacquemond, V., Mariol, M.C., Segalat, L., and Allard, B. (2002). The L-type voltage-dependent Ca2+ channel EGL-19 controls body wall muscle function in Caenorhabditis elegans. J Cell Biol *159*, 337-348.

Katz, P.S. (1998). Neuromodulation intrinsic to the central pattern generator for escape swimming in Tritonia. Annals of the New York Academy of Sciences *860*, 181-188.

Kerr, R., Lev-Ram, V., Baird, G., Vincent, P., Tsien, R.Y., and Schafer, W.R. (2000). Optical imaging of calcium transients in neurons and pharyngeal muscle of C. elegans. Neuron *26*, 583-594.

Kerr, R.A. (2006). Imaging the activity of neurons and muscles (The *C. elegans* Research Community).

Kim, J., Poole, D.S., Waggoner, L.E., Kempf, A., Ramirez, D.S., Treschow, P.A., and Schafer, W.R. (2001). Genes affecting the activity of nicotinic receptors involved in Caenorhabditis elegans egg-laying behavior. Genetics *157*, 1599-1610.

Kim, K., and Li, C. (2004). Expression and regulation of an FMRFamide-related neuropeptide gene family in Caenorhabditis elegans. J Comp Neurol *475*, 540-550.

Koelle, M.R., and Horvitz, H.R. (1996). Egl-10 regulates G-protein signaling in the *C. elegans* nervous system and shares a conserved domain with many mammalian proteins. Cell *84*, 115-125.

Koushika, S.P., Richmond, J.E., Hadwiger, G., Weimer, R.M., Jorgensen, E.M., and Nonet, M.L. (2001). A post-docking role for active zone protein Rim. Nat Neurosci *4*, 997-1005.

Lee, J.H., Cribbs, L.L., and Perez-Reyes, E. (1999). Cloning of a novel four repeat protein related to voltage-gated sodium and calcium channels. FEBS Lett *445*, 231-236.

Lee, R.Y., Lobel, L., Hengartner, M., Horvitz, H.R., and Avery, L. (1997a). Mutations in the alpha1 subunit of an L-type voltage-activated Ca2+ channel cause myotonia in Caenorhabditis elegans. Embo J *16*, 6066-6076.

Lee, R.Y.N., Lobel, L., Hengartner, M., Horvitz, H.R., and Avery, L. (1997b). Mutations in the α1 subunit of an L-type voltage-activated Ca^{2+} channel cause myotonia in Caenorhabditis elegans. EMBO J. *16*, 6066-6076.

Lesch, K.P. (2005). Alcohol dependence and gene x environment interaction in emotion regulation: Is serotonin the link? European journal of pharmacology *526*, 113-124.

Li, C., and Chalfie, M. (1990). Organogenesis in C. elegans: positioning of neurons and muscles in the egg-laying system. Neuron *4*, 681-695.

Llinas, R.R. (1988). The intrinsic electrophysiological properties of mammalian neurons: insights into central nervous system function. Science *242*, 1654-1664.

Lu, B., Su, Y., Das, S., Liu, J., Xia, J., and Ren, D. (2007). The neuronal channel NALCN contributes resting sodium permeability and is required for normal respiratory rhythm. Cell *129*, 371-383.

Marder, E., Bucher, D., Schulz, D.J., and Taylor, A.L. (2005). Invertebrate central pattern generation moves along. Curr Biol *15*, R685-699.

Mathews, E.A., Garcia, E., Santi, C.M., Mullen, G.P., Thacker, C., Moerman, D.G., and Snutch, T.P. (2003). Critical residues of the Caenorhabditis elegans unc-2 voltage-gated calcium channel that affect behavioral and physiological properties. J Neurosci *23*, 6537-6545.

Nash, H.A., Scott, R.L., Lear, B.C., and Allada, R. (2002). An unusual cation channel mediates photic control of locomotion in Drosophila. Curr Biol *12*, 2152-2158.

Nathoo, A.N., Moeller, R.A., Westlund, B.A., and Hart, A.C. (2001). Identification of neuropeptide-like protein gene families in Caenorhabditiselegans and other species.

Proceedings of the National Academy of Sciences of the United States of America *98*, 14000-14005.

Nishimune, H., Sanes, J.R., and Carlson, S.S. (2004). A synaptic laminin-calcium channel interaction organizes active zones in motor nerve terminals. Nature *432*, 580-587.

Nusbaum, M.P., and Beenhakker, M.P. (2002). A small-systems approach to motor pattern generation. Nature *417*, 343-350.

Patel, M.R., Lehrman, E.K., Poon, V.Y., Crump, J.G., Zhen, M., Bargmann, C.I., and Shen, K. (2006). Hierarchical assembly of presynaptic components in defined C. elegans synapses. Nat Neurosci *9*, 1488-1498.

Pieribone, V.A., Porton, B., Rendon, B., Feng, J., Greengard, P., and Kao, H.T. (2002). Expression of synapsin III in nerve terminals and neurogenic regions of the adult brain. J Comp Neurol *454*, 105-114.

Pietrobon, D. (2005). Function and dysfunction of synaptic calcium channels: insights from mouse models. Curr Opin Neurobiol *15*, 257-265.

Reigl, M., Alon, U., and Chklovskii, D.B. (2004). Search for computational modules in the C. elegans brain. BMC biology *2*, 25.

Reiner, D.J., Weinshenker, D., and Thomas, J.H. (1995). Analysis of dominant mutations affecting muscle excitation in *Caenorhabditis elegans*. Genetics *141*, 961-976.

Richmond, J.E., Davis, W.S., and Jorgensen, E.M. (1999). UNC-13 is required for synaptic vesicle fusion in C. elegans. Nature neuroscience *2*, 959-964.

Richmond, J.E., and Jorgensen, E.M. (1999). One GABA and two acetylcholine receptors function at the C. elegans neuromuscular junction. Nat Neurosci *2*, 791-797.

Sather, W.A., and McCleskey, E.W. (2003). Permeation and selectivity in calcium channels. Annu Rev Physiol *65*, 133-159.

Sawin, E.R. (1996). Genetic and cellular analysis of modulated behaviors in *Caenorhabditis elegans*. In Biology (Cambridge, MA, M. I. T.).

Schafer, W.F. (2006). Genetics of egg-laying in worms. Annu Rev Genet *40*, 487-509.

Schafer, W.R., and Kenyon, C.J. (1995). A calcium-channel homologue required for adaptation to dopamine and serotonin in Caenorhabditis elegans. Nature *375*, 73-78.

Schafer, W.R., Sanchez, B.M., and Kenyon, C.J. (1996). Genes affecting sensitivity to serotonin in Caenorhabditis elegans. Genetics *143*, 1219-1230.

Schinkmann, K., and Li, C. (1992). Localization of FMRFamide-like peptides in *Caenorhaditis elegans*. J. Comp. Neurol. *316*, 251-260.

Schlief, T., Schonherr, R., Imoto, K., and Heinemann, S.H. (1996). Pore properties of rat brain II sodium channels mutated in the selectivity filter domain. Eur Biophys J *25*, 75-91.

Sedensky, M.M., and Meneely, P.M. (1987). Genetic analysis of halothane sensitivity in Caenorhabditis elegans. Science *236*, 952-954.

Selverston, A.I. (2005). A neural infrastructure for rhythmic motor patterns. Cellular and molecular neurobiology *25*, 223-244.

Shen, N., Datta, D., Schaffer, C.B., LeDuc, P., Ingber, D.E., and Mazur, E. (2005). Ablation of cytoskeletal filaments and mitochondria in live cells using a femtosecond laser nanoscissor. Mech Chem Biosyst *2*, 17-25.

Shtonda, B., and Avery, L. (2005). CCA-1, EGL-19 and EXP-2 currents shape action potentials in the Caenorhabditis elegans pharynx. J Exp Biol *208*, 2177-2190.

Shyn, S.I., Kerr, R., and Schafer, W.R. (2003). Serotonin and Go modulate functional states of neurons and muscles controlling C. elegans egg-laying behavior. Curr Biol *13*, 1910-1915.

Sieburth, D., Ch'ng, Q., Dybbs, M., Tavazoie, M., Kennedy, S., Wang, D., Dupuy, D., Rual, J.F., Hill, D.E., Vidal, M., *et al.* (2005). Systematic analysis of genes required for synapse structure and function. Nature *436*, 510-517.

Siegel, M.S., and Isacoff, E.Y. (1997). A genetically encoded optical probe of membrane voltage. Neuron *19*, 735-741.

Song, S., Sjostrom, P.J., Reigl, M., Nelson, S., and Chklovskii, D.B. (2005). Highly nonrandom features of synaptic connectivity in local cortical circuits. PLoS biology *3*, e68.

Steger, K.A., Shtonda, B.B., Thacker, C., Snutch, T.P., and Avery, L. (2005). The C. elegans T-type calcium channel CCA-1 boosts neuromuscular transmission. J Exp Biol *208*, 2191-2203.

Suzuki, H., Kerr, R., Bianchi, L., Frokjaer-Jensen, C., Slone, D., Xue, J., Gerstbrein, B., Driscoll, M., and Schafer, W.R. (2003). In vivo imaging of C. elegans mechanosensory neurons demonstrates a specific role for the MEC-4 channel in the process of gentle touch sensation. Neuron *39*, 1005-1017.

Sze, J.Y., Victor, M., Loer, C., Shi, Y., and Ruvkun, G. (2000). Food and metabolic signaling defects in a *Caenorhabditis elegans* serotonin-synthesis mutant. Nature *403*, 560-564.

Tam, T., Mathews, E., Snutch, T.P., and Schafer, W.R. (2000). Voltage-gated calcium channels direct neuronal migration in Caenorhabditis elegans. Dev Biol *226*, 104-117.

Touroutine, D., Fox, R.M., Von Stetina, S.E., Burdina, A., Miller, D.M., 3rd, and Richmond, J.E. (2005). acr-16 encodes an essential subunit of the levamisole-resistant nicotinic receptor at the Caenorhabditis elegans neuromuscular junction. J Biol Chem *280*, 27013-27021.

Trent, C., Tsung, N., and Horvitz, H.R. (1983). Egg-laying defective mutants of the nematode *Caenorhabditis elegans*. Genetics *104*, 619-647.

Truong, K., Sawano, A., Miyawaki, A., and Ikura, M. (2007). Calcium indicators based on calmodulin-fluorescent protein fusions. Methods Mol Biol *352*, 71-82.

Tsutsui, H., Wolf, A.M., Knopfel, T., and Oka, Y. (2001). Imaging postsynaptic activities of teleost thalamic neurons at single cell resolution using a voltage-sensitive dye. Neurosci Lett *312*, 17-20.

Vinogradova, I., Cook, A., and Holden-Dye, L. (2006). The ionic dependence of voltage-activated inward currents in the pharyngeal muscle of Caenorhabditis elegans. Invert Neurosci *6*, 57-68.

Waggoner, L., Zhou, G.T., Schafer, R.W., and Schafer, W.R. (1998a). Control of behavioral states by serotonin in *Caenorhabditis elegans*. Neuron *21*, 203-214.

Waggoner, L.E., Dickinson, K.A., Poole, D.S., Tabuse, Y., Miwa, J., and Schafer, W.R. (2000a). Long-term nicotine adaptation in *Caenorhabditis elegans* involves PKC-dependent changes in nicotinic receptor abundance. J. Neurosci *20*, 8802-8811.

Waggoner, L.E., Hardaker, L.A., Golik, S., and Schafer, W.R. (2000b). Effect of a neuropeptide gene on behavioral states in *Caenorhabditis elegans* egg-laying. Genetics *154*, 1181-1192.

Waggoner, L.E., Zhou, G.T., Schafer, R.W., and Schafer, W.R. (1998b). Control of alternative behavioral states by serotonin in Caenorhabditis elegans. Neuron *21*, 203-214.

White, J., Southgate, E., Thomson, N., and Brenner, S. (1986). The structure of the *Caenorhabditis elegans* nervous system. Philos. Trans. R. Soc. Lond. (Biol.) *314*, 1-340.

White, J.G., Southgate, E., Thomson, J.N., Brenner, S. (1986). The Structure of the Nervous System of the Nematode Caenorhabditis elegans., Vol 314.

Yang, J., Ellinor, P.T., Sather, W.A., Zhang, J.F., and Tsien, R.W. (1993). Molecular determinants of Ca2+ selectivity and ion permeation in L-type Ca2+ channels. Nature *366*, 158-161.

Yanik, M.F., Cinar, H., Cinar, H.N., Chisholm, A.D., Jin, Y., and Ben-Yakar, A. (2004). Neurosurgery: functional regeneration after laser axotomy. Nature *432*, 822.

Yarom, Y., Sugimori, M., and Llinas, R. (1985). Ionic currents and firing patterns of mammalian vagal motoneurons in vitro. Neuroscience *16*, 719-737.

Yeh, E., Kawano, T., Weimer, R.M., Bessereau, J.L., and Zhen, M. (2005). Identification of genes involved in synaptogenesis using a fluorescent active zone marker in Caenorhabditis elegans. J Neurosci *25*, 3833-3841.

Yu, F.H., and Catterall, W.A. (2003). Overview of the voltage-gated sodium channel family. Genome Biol *4*, 207.

Zhang, F., Wang, L.P., Brauner, M., Liewald, J.F., Kay, K., Watzke, N., Wood, P.G., Bamberg, E., Nagel, G., Gottschalk, A., and Deisseroth, K. (2007). Multimodal fast optical interrogation of neural circuitry. Nature *446*, 633-639.

Zhang, J., Ma, Y., Taylor, S.S., and Tsien, R.Y. (2001). Genetically encoded reporters of protein kinase A activity reveal impact of substrate tethering. Proceedings of the National Academy of Sciences of the United States of America *98*, 14997-15002.

Zhen, M., and Jin, Y. (1999). The liprin protein SYD-2 regulates the differentiation of presynaptic termini in C. elegans. Nature *401*, 371-375.

Zhou, G.T., Schafer, W.R., and Schafer, R.W. (1998). A three-state biological point process model and its parameter estimation. IEEE Trans. on Signal Processing *46*, 2698-2707.